

CONVERGENCE ANALYSIS OF NEURAL NETWORKS FOR SOLVING A FREE BOUNDARY PROBLEM

XINYUE EVELYN ZHAO, WENRUI HAO, AND BEI HU

ABSTRACT. Free boundary problems deal with systems of partial differential equations, where the domain boundary is apriori unknown. Due to this special characteristic, it is challenging to solve the free boundary problems either theoretically or numerically. In this paper, we develop a novel approach for solving a modified Hele-Shaw problem based on the neural network discretization. The existence of the numerical solution with this discretization is established theoretically. We also numerically verify this approach by computing the symmetry-breaking solutions that are guided by the bifurcation analysis near the radially-symmetric branch. Moreover, we further verify the capability of this approach by computing some non-radially symmetric solutions which are not characterized by any theorems.

1. INTRODUCTION

Many mathematical models of natural phenomena, e.g., biology, physics and materials science, involve the solution of systems of partial differential equations (PDEs) with free (moving) boundaries [1–5]. Among these free boundary problems, the generalized Hele-Shaw problem with surface tension is the most popular and widely-studied problem with various applications ranging from physics to biology [1, 6]. This problem has attracted extensive experimental and mathematical studies since the initial work of Saffman and Taylor in 1958 [7], based on the experimental innovation of confining a fluid between two closely-spaced plates by Hele-Shaw [8]. From a mathematical point of view, studies of this problem can be formulated both numerically and theoretically to focus on the solutions and their structures [9, 10]. In the last few decades, generalized Hele-Shaw problems with surface tension have been formulated from biological and physical modeling [1, 11]. Thus theories and nonlinear simulations of these problems have been developed to understand the structure of steady-state solutions. Although the PDE theory can help in some special cases, the in-depth study of these problems often requires large-scale simulations including numerically computing steady-state solutions [5, 12]. Efficient numerical methods for computing the steady-state solutions [13], bifurcations [14], and stability are keys to understanding these systems. Underlying all these is the common grand challenge of developing efficient numerical algorithms for complex PDE systems with free (moving) boundaries.

Recently, there are several numerical methods developed for studying the generalized Hele-Shaw problem with surface tension, e.g., computing multiple steady-states by coupling multi-grid and domain decomposition techniques with numerical algebraic geometry [5, 12, 13, 15]; detecting bifurcation points by using the adaptive homotopy tracking method [14, 16, 17]; and exploring their global solution structures based on PDE theories [5, 14, 18]. These numerical methods have also been successfully applied to some complex biological networks including tumor growth model and cardiovascular disease risk evaluation [3, 4]. We also analyzed the boundary integral method on a simplified Hele-Shaw problem without the surface tension term [18] and provided a rigorous convergence analysis. However, to the date, there are still several numerical challenges for solving the generalized Hele-Shaw problem with surface tension:

- 1) there is lack of rigorous theoretical analysis of numerical methods for free boundary problems with the surface tension;
- 2) and steady-state solution patterns are hard to compute so that the global solution structure is unclear.

Therefore, efficient numerical methods, rigorous theoretical analysis of these numerical methods and global solution structures are needed to deeply study for the generalized Hele-Shaw problem.

Machine learning has been experiencing an extraordinary resurgence in many important artificial intelligence applications since the late 2000s. In particular, it has been able to produce state-of-the-art accuracy in computer vision [19], video analysis [20], natural language processing [21] and speech recognition [22]. Recently, interest in machine learning based approaches in the applied mathematics

community has increased rapidly [23, 24]. This growing enthusiasm for machine learning stems from massive amounts of data available from scientific computations [25] and other sources [26]; the design of efficient data analysis algorithms [27]; advances in high-performance computing; and the data-driven modeling [28]. In order to take advantage of machine learning, we will develop a new approach for solving free boundary problems and address the current challenges in this area.

2. THE FREE BOUNDARY PROBLEM AND BIFURCATION ANALYSIS

2.1. The model problem. The classical Hele-Shaw problem seeks a fluid domain $\Omega(t) \in \mathbb{R}^2$ and the fluid pressure σ such that

$$(2.1) \quad \begin{cases} \Delta\sigma = 0 & \text{in } \Omega(t), \\ \sigma = \kappa & \text{on } \partial\Omega(t), \\ V_n = -\frac{\partial\sigma}{\partial\mathbf{n}} & \text{on } \partial\Omega(t), \end{cases}$$

where κ denotes the curvature of $\partial\Omega(t)$ ($\kappa = \frac{1}{R}$ if $\partial\Omega(t)$ is a circle of radius $R > 0$); and V_n is the velocity of the fluid boundary $\partial\Omega(t)$ in the outward normal direction \mathbf{n} .

It is well-known that model (2.1) possesses only radially symmetric stationary solution. In order to investigate the complexity of free boundaries, we introduce a modified Hele-Shaw model as below:

$$(2.2) \quad \begin{cases} -\Delta\sigma = c(-\sigma - \mu) & \text{in } \Omega(t), \\ \sigma = \kappa & \text{on } \partial\Omega(t), \\ V_n = -\frac{\partial\sigma}{\partial\mathbf{n}} + \beta & \text{on } \partial\Omega(t), \end{cases}$$

where $c, \mu, \beta > 0$. The first equation on the right-hand side of (2.2) represents a sink of fluid, while the additional constant β represents the influx of fluid in addition to the balance of mass. When $c = \beta = 0$, (2.2) reverts to the classical Hele-Shaw problem. By introducing the non-dimensional length scale $L_D = \sqrt{c}$, we define:

$$\tilde{\mathbf{x}} = L_D \mathbf{x}, \quad \tilde{\sigma}(\tilde{\mathbf{x}}) = \sigma(\mathbf{x}) + \mu, \quad \tilde{\Omega}(t) = L_D \Omega(t), \quad \tilde{\beta} = \frac{\beta}{L_D}.$$

After dropping the \sim in the above variables, the non-dimensional model takes the following form

$$(2.3) \quad \begin{cases} -\Delta\sigma = -\sigma & \text{in } \Omega(t), \\ \sigma = \mu + \kappa & \text{on } \partial\Omega(t), \\ V_n = -\frac{\partial\sigma}{\partial\mathbf{n}} + \beta & \text{on } \partial\Omega(t), \end{cases}$$

We consider the steady state system of (2.3) by setting $V_n = 0$ and obtain the system for σ :

$$(2.4) \quad \begin{cases} -\Delta\sigma = -\sigma & \text{in } \Omega, \\ \sigma = \mu + \kappa & \text{on } \partial\Omega, \\ \frac{\partial\sigma}{\partial\mathbf{n}} = \beta & \text{on } \partial\Omega. \end{cases}$$

Theoretically, system (2.4) admits a unique radially symmetric solution $\sigma_S(r)$ with radius $r = R_S$:

$$(2.5) \quad \sigma_S(r) = \left(\mu + \frac{1}{R_S}\right) \frac{I_0(r)}{I_0(R_S)},$$

provided that $\beta = \beta(\mu, R_S)$ is given by

$$(2.6) \quad \beta = \left(\mu + \frac{1}{R_S}\right) \frac{I_1(R_S)}{I_0(R_S)}.$$

Here $I_n(r)$ is the modified Bessel function for integer $n \geq 0$.

We are more interested in finding the non-radially symmetric solutions of system (2.4). Particularly, we would like to know what the boundaries look like in non-radially symmetric case. In this section, we shall carry out a theoretical bifurcation analysis by using the Crandall Rabinowitz Theorem (Theorem 8.1 in Appendix) to show there exists branches of symmetry-breaking solutions to system (2.4); and in the next section, we will propose a new method, which is a combination of boundary integral method (BIM) and machine learning approximation, to numerically derive the shapes of the boundaries of system (2.4).

2.2. Bifurcation results. To begin with, we consider a family of domains with perturbed boundaries in polar coordinates

$$\partial\Omega_\varepsilon : r = R_S + \tilde{R}(\theta) = R_S + \varepsilon S(\theta).$$

Let σ be the solution of the system

$$(2.7) \quad \begin{cases} -\Delta\sigma = -\sigma & \text{in } \Omega_\varepsilon, \\ \sigma = \mu + \kappa & \text{on } \partial\Omega_\varepsilon, \end{cases}$$

and define \mathcal{F} by

$$(2.8) \quad \mathcal{F}(\tilde{R}, \mu) = \frac{\partial\sigma}{\partial\mathbf{n}} \Big|_{\partial\Omega_\varepsilon} - \beta.$$

Based on system (2.4), σ is a symmetry-breaking solution of system (2.4) if and only if $\mathcal{F}(\tilde{R}, \mu) = 0$.

Following [29–34], it can be established that σ admits the following expansion

$$(2.9) \quad \sigma = \sigma_S + \varepsilon\sigma_1 + O(\varepsilon^2),$$

where σ_1 is the solution to the linearized system (B_{R_S} denotes the disk centered at 0 with radius R_S)

$$(2.10) \quad \begin{cases} -\Delta\sigma_1 = -\sigma_1 & \text{in } B_{R_S}, \\ \sigma_1 = -\frac{1}{R_S^2}(S + S_{\theta\theta}) - \frac{\partial\sigma_S(R_S)}{\partial r}S & \text{on } \partial B_{R_S}. \end{cases}$$

We then substitute (2.9) into (2.8) to obtain

$$\begin{aligned} \mathcal{F}(\tilde{R}, \mu) &= \frac{\partial\sigma_S(R_S)}{\partial r} + \frac{\partial^2\sigma_S(R_S)}{\partial r^2}\varepsilon S(\theta) + \frac{\partial\sigma_1(R_S, \theta)}{\partial r}\varepsilon - \beta + O(\varepsilon^2) \\ &= \mathcal{F}(0, \mu) + \varepsilon\left(\frac{\partial^2\sigma_S(R_S)}{\partial r^2}S(\theta) + \frac{\partial\sigma_1(R_S, \theta)}{\partial r}\right) + O(\varepsilon^2), \end{aligned}$$

which formally gives the Fréchet derivative of \mathcal{F} as:

$$(2.11) \quad [\mathcal{F}_{\tilde{R}}(0, \mu)]S(\theta) = \frac{\partial^2\sigma_S(R_S)}{\partial r^2}S(\theta) + \frac{\partial\sigma_1(R_S, \theta)}{\partial r}.$$

In what follows, we shall use (2.11) to establish the bifurcation points by verifying the regularity and the four assumptions in the Crandall-Rabinowitz Theorem.

Like in [34], we introduce the Banach spaces:

$$X^{l+\alpha} = \{S \in C^{l+\alpha}(B_1), S \text{ is } 2\pi\text{-periodic in } \theta\},$$

$$X_2^{l+\alpha} = \text{closure of the linear space spanned by } \{\cos(n\theta), n = 0, 2, 4, \dots\} \text{ in } X^{l+\alpha},$$

and set the perturbation $S(\theta) = \cos(n\theta)$. Using a separation of variables, we seek a solution of the form

$$(2.12) \quad \sigma_1(r, \theta) = \sigma_1^n(r) \cos(n\theta).$$

Based on (2.10), σ_1^n satisfies

$$(2.13) \quad \begin{cases} -\frac{\partial^2\sigma_1^n}{\partial r^2} - \frac{1}{r}\frac{\partial\sigma_1^n}{\partial r} + \frac{n^2}{r^2}\sigma_1^n = -\sigma_1^n & \text{in } B_{R_S}, \\ \sigma_1^n = \frac{n^2-1}{R_S^2} - \frac{\partial\sigma_S(R_S)}{\partial r} & \text{on } \partial B_{R_S}, \end{cases}$$

and is explicitly given by

$$(2.14) \quad \sigma_1^n(r) = \left[\frac{n^2-1}{R_S^2} - \frac{\partial\sigma_S(R_S)}{\partial r} \right] \frac{I_n(r)}{I_n(R_S)} = \left[\frac{n^2-1}{R_S^2} - \left(\mu + \frac{1}{R_S} \right) \frac{I_1(R_S)}{I_0(R_S)} \right] \frac{I_n(r)}{I_n(R_S)}.$$

Substituting (2.5), (2.12), and (2.14) into (2.11), we obtain

$$\begin{aligned} [\mathcal{F}_{\tilde{R}}(0, \mu)] \cos(n\theta) &= \left[\left(\mu + \frac{1}{R_S} \right) \frac{I'_1(R_S)}{I_0(R_S)} + \left[\frac{n^2-1}{R_S^2} - \left(\mu + \frac{1}{R_S} \right) \frac{I_1(R_S)}{I_0(R_S)} \right] \frac{I'_n(R_S)}{I_n(R_S)} \right] \cos(n\theta) \\ (2.15) \quad &= \left[-\mu \frac{I_1(R_S)}{I_0(R_S)} \left(\frac{I'_n(R_S)}{I_n(R_S)} - \frac{I'_1(R_S)}{I_1(R_S)} \right) \right. \\ &\quad \left. + \frac{n^2-1}{R_S^2} \frac{I'_n(R_S)}{I_n(R_S)} - \frac{I_1(R_S)}{R_S I_0(R_S)} \left(\frac{I'_n(R_S)}{I_n(R_S)} - \frac{I'_1(R_S)}{I_1(R_S)} \right) \right] \cos(n\theta). \end{aligned}$$

It follows that for $n \neq 1$, $[\mathcal{F}_{\tilde{R}}(0, \mu)] \cos(n\theta) = 0$ if and only if

$$\begin{aligned}
 \mu &= \mu_n(R_S) \\
 &\triangleq \left[\frac{n^2 - 1}{R_S^2} \frac{I'_n(R_S)}{I_n(R_S)} - \frac{I_1(R_S)}{R_S I_0(R_S)} \left(\frac{I'_n(R_S)}{I_n(R_S)} - \frac{I'_1(R_S)}{I_1(R_S)} \right) \right] / \left[\frac{I_1(R_S)}{I_0(R_S)} \left(\frac{I'_n(R_S)}{I_n(R_S)} - \frac{I'_1(R_S)}{I_1(R_S)} \right) \right] \\
 (2.16) \quad &= -\frac{1}{R_S} + \frac{I_0(R_S)}{R_S^2 I_1(R_S)} \cdot \left[(n^2 - 1) \frac{I'_n(R_S)}{I_n(R_S)} \right] / \left[\frac{I'_n(R_S)}{I_n(R_S)} - \frac{I'_1(R_S)}{I_1(R_S)} \right] \\
 &= -\frac{1}{R_S} + \frac{I_0(R_S)}{R_S^2 I_1(R_S)} \cdot \frac{I'_n(R_S)}{I_n(R_S)} / \left[\frac{1}{n^2 - 1} \left(\frac{I'_n(R_S)}{I_n(R_S)} - \frac{I'_1(R_S)}{I_1(R_S)} \right) \right].
 \end{aligned}$$

In order to analyze μ_n , we recall two inequalities from [35], namely,

$$([7, (A.1)]) \quad \frac{I'_{n+1}(r)}{I_{n+1}(r)} > \frac{I'_n(r)}{I_n(r)} \quad \text{for all } n \geq 0 \text{ and } r > 0,$$

$$([7, (A.7)]) \quad \frac{1}{n^2 - 1} \left(\frac{I'_n(r)}{I_n(r)} - \frac{I'_1(r)}{I_1(r)} \right) > \frac{1}{(n+1)^2 - 1} \left(\frac{I'_{n+1}(r)}{I_{n+1}(r)} - \frac{I'_1(r)}{I_1(r)} \right) \quad \text{for all } n \geq 2 \text{ and } r > 0;$$

based on these two inequalities, we have, for $n \geq 2$,

$$\mu_{n+1} > \mu_n.$$

Moreover, the same proof from [35] can easily be modified to establish

$$\frac{1}{0^2 - 1} \left(\frac{I'_0(r)}{I_0(r)} - \frac{I'_1(r)}{I_1(r)} \right) > \frac{1}{2^2 - 1} \left(\frac{I'_2(r)}{I_2(r)} - \frac{I'_1(r)}{I_1(r)} \right),$$

together with [35, (A.1)], we also have

$$\mu_2 > \mu_0.$$

On the other hand, using $I'_0(r) = I_1(r)$ and $I'_1(r) = I_2(r) + \frac{1}{r} I_1(r)$, we simplify μ_0 as

$$\begin{aligned}
 \mu_0 &= \frac{1}{R_S} \left[-1 + \frac{I_0(R_S) I_1(R_S)}{R_S I_0(R_S) I_2(R_S) + I_0(R_S) I_1(R_S) - R_S I_1^2(R_S)} \right] \\
 &= \frac{1}{R_S} \left[-1 + 1 / \left(R_S \frac{I_2(R_S)}{I_1(R_S)} - R_S \frac{I_1(R_S)}{I_0(R_S)} + 1 \right) \right].
 \end{aligned}$$

Since $I_0(R_S) I_2(R_S) < I_1^2(R_S)$, we get $\frac{I_2(R_S)}{I_1(R_S)} < \frac{I_1(R_S)}{I_0(R_S)}$, which implies $R_S \frac{I_2(R_S)}{I_1(R_S)} - R_S \frac{I_1(R_S)}{I_0(R_S)} + 1 < 1$. Moreover, by [35, (A.1)], $\frac{I'_1(R_S)}{I_1(R_S)} - \frac{I'_0(R_S)}{I_0(R_S)} = \frac{I_2(R_S)}{I_1(R_S)} - \frac{1}{R_S} - \frac{I_1(R_S)}{I_0(R_S)} > 0$, so that $R_S \frac{I_2(R_S)}{I_1(R_S)} - R_S \frac{I_1(R_S)}{I_0(R_S)} + 1 > 0$. Hence it is clear that $\mu_0 > 0$. Putting these estimates all together, we have, for $n \geq 2$,

$$(2.17) \quad 0 < \mu_0 < \mu_2 < \mu_3 < \mu_4 < \dots$$

With this monotonicity of μ_n , we are now able to establish the bifurcation result for system (2.4).

We choose $X = X_2^{3+\alpha}$ and $Y = X_2^\alpha$ in the Crandall-Rabinowitz Theorem. The rigorous justifications of the Fréchet derivative and differentiability of \mathcal{F} follow from the same arguments as those in [29–34]. We now proceed to verify the four assumptions of the theorem. The assumption (1) is naturally satisfied. Due to (2.17), the kernel space satisfies

$$\text{Ker}[\mathcal{F}_{\tilde{R}}(0, \mu_n)] = \text{span}\{\cos(n\theta)\} \quad \text{for even } n \geq 2,$$

which indicates

$$\dim(\text{Ker}[\mathcal{F}_{\tilde{R}}(0, \mu_n)]) = 1 \quad \text{for even } n \geq 2.$$

Moreover, since $\text{Im}[\mathcal{F}_{\tilde{R}}(0, \mu_n)] \oplus \text{span}\{\cos(n\theta)\} = Y$ is the whole space, we have $\text{codim}(\text{Im}[\mathcal{F}_{\tilde{R}}(0, \mu_n)]) = 1$. Finally, by differentiating (2.15) with respect to μ , we obtain

$$[\mathcal{F}_{\mu \tilde{R}}(0, \mu_n)] \cos(n\theta) = -\frac{I_1(R_S)}{I_0(R_S)} \left(\frac{I'_n(R_S)}{I_n(R_S)} - \frac{I'_1(R_S)}{I_1(R_S)} \right) \cos(n\theta) \notin \text{Im}[\mathcal{F}_{\tilde{R}}(0, \mu_n)].$$

Thus all the assumptions in the Crandall-Rabinowitz Theorem are satisfied, and the following bifurcation result for system (2.4) is established.

Theorem 2.1. *For each even $n \geq 2$, $\mu = \mu_n(R_S)$ is a bifurcation point of the symmetry-breaking solution to the system (2.4) with free boundary*

$$(2.18) \quad r = R_s + \varepsilon \cos(n\theta) + o(\varepsilon), \quad \mu = \mu(\varepsilon) = \mu_n(R_S) + o(1).$$

Remark 2.1. *The bifurcation result is actually valid for all $n \geq 2$ not restricting to even n only, however the proof is much more complicated.*

3. THE NUMERICAL METHOD BASED ON THE NEURAL NETWORK DISCRETIZATION

3.1. Boundary integral formulation. Using the boundary integral formulation [36–39], we apply the standard representation formula [40] on system (2.4) to obtain

$$(3.1) \quad \sigma(\mathbf{x}) = \int_{\partial\Omega} \left[G_1(\mathbf{x}, \mathbf{y}) \frac{\partial \sigma(\mathbf{y})}{\partial \mathbf{n}_y} - \sigma(\mathbf{y}) \frac{\partial G_1(\mathbf{x}, \mathbf{y})}{\partial \mathbf{n}_y} \right] dS_y \quad \text{for } \mathbf{x} \in \Omega,$$

where G_1 is the Green function for the operator $-\Delta + 1$, namely, $G_1(\mathbf{x}, \mathbf{y}) = G_1(|\mathbf{x} - \mathbf{y}|) = \frac{i}{4} H_0^{(1)}(i|\mathbf{x} - \mathbf{y}|)$ for two dimensional case, and $H_0^{(1)}$ is a Hankel function. By using the “jump” relationship [41] as $\mathbf{x} \rightarrow \partial\Omega$, we derive

$$(3.2) \quad \frac{\sigma(\mathbf{x})}{2} = \int_{\partial\Omega} \left[G_1(\mathbf{x}, \mathbf{y}) \frac{\partial \sigma(\mathbf{y})}{\partial \mathbf{n}_y} - \sigma(\mathbf{y}) \frac{\partial G_1(\mathbf{x}, \mathbf{y})}{\partial \mathbf{n}_y} \right] dS_y \quad \text{for } \mathbf{x} \in \partial\Omega.$$

Combining with the boundary conditions in (2.4), we further obtain

$$(3.3) \quad \frac{\mu + \kappa(\mathbf{x})}{2} = \int_{\partial\Omega} \left[\beta G_1(\mathbf{x}, \mathbf{y}) - (\mu + \kappa(\mathbf{y})) \frac{\partial G_1(\mathbf{x}, \mathbf{y})}{\partial \mathbf{n}_y} \right] dS_y \quad \text{for } \mathbf{x} \in \partial\Omega.$$

Since the function $G_1(r)$ and $G_1'(r)$ are singular at $r = 0$, we introduce a new function $Q(r)$ defined as

$$(3.4) \quad Q(r) = \frac{1}{r} \left(G_1'(r) + \frac{1}{2\pi r} \right).$$

Then $Q(r) = O(|\ln r|)$, $Q'(r) = O(r^{-1})$, $Q''(r) = O(r^{-2})$ (see [42]). As in [42], if we replace G_1 in (3.2) by the fundamental solution for $-\Delta$ (which equals to $-\frac{1}{2\pi} \ln |\mathbf{x} - \mathbf{y}|$), and take $\sigma = 1$, we have

$$(3.5) \quad \frac{1}{2} = - \int_{\partial\Omega} \frac{\partial}{\partial \mathbf{n}_y} \left(-\frac{1}{2\pi} \ln |\mathbf{x} - \mathbf{y}| \right) dS_y = \frac{1}{2\pi} \int_{\partial\Omega} \frac{\mathbf{y} - \mathbf{x}}{|\mathbf{x} - \mathbf{y}|^2} \cdot \mathbf{n}_y dS_y \quad \text{for } \mathbf{x} \in \partial\Omega,$$

hence

$$(3.6) \quad \frac{\mu + \kappa(\mathbf{x})}{2} = \frac{1}{2\pi} \int_{\partial\Omega} (\mu + \kappa(\mathbf{x})) \frac{\mathbf{y} - \mathbf{x}}{|\mathbf{x} - \mathbf{y}|^2} \cdot \mathbf{n}_y dS_y \quad \text{for } \mathbf{x} \in \partial\Omega.$$

Using (3.4), (3.5), as well as (3.6), we can rewrite (3.3) as

$$(3.7) \quad \int_{\partial\Omega} \left[\beta G_1(\mathbf{x}, \mathbf{y}) - \left((\mu + \kappa(\mathbf{y})) Q(|\mathbf{x} - \mathbf{y}|) - \frac{\kappa(\mathbf{y}) - \kappa(\mathbf{x})}{2\pi |\mathbf{x} - \mathbf{y}|^2} \right) (\mathbf{y} - \mathbf{x}) \cdot \mathbf{n}_y \right] dS_y = 0 \quad \text{for } \mathbf{x} \in \partial\Omega,$$

with $\partial\Omega$ being the only unknown in the equation.

Equation (3.7) determines the free boundary $\partial\Omega$. Due to the highly non-linear nature of (3.7), there might be multiple solutions of $\partial\Omega$. These solutions are expected to be computed by the machine learning techniques.

3.2. The neural network discretization. We use $\partial\Omega : r = R(\theta)$, $\theta \in (-\infty, \infty)$ to represent the unknown boundary. Clearly, it satisfies the 2π -periodic boundary condition, namely,

$$(3.8) \quad R(\theta) = R(\theta + 2\pi).$$

For simplicity, we shall restrict θ to $[0, 2\pi]$. By denoting in the polar coordinates $\mathbf{x} = (R(\hat{\theta}) \cos(\hat{\theta}), R(\hat{\theta}) \sin(\hat{\theta}))$ and $\mathbf{y} = (R(\theta) \cos(\theta), R(\theta) \sin(\theta))$, we have

$$\begin{aligned} |\mathbf{x} - \mathbf{y}| &= \sqrt{[R(\hat{\theta}) \cos(\hat{\theta}) - R(\theta) \cos(\theta)]^2 + [R(\hat{\theta}) \sin(\hat{\theta}) - R(\theta) \sin(\theta)]^2} \\ &= \sqrt{R^2(\hat{\theta}) + R^2(\theta) - 2R(\hat{\theta})R(\theta) \cos(\hat{\theta} - \theta)} \\ &\triangleq D[R]. \end{aligned}$$

In addition,

$$\begin{aligned} \mathbf{n}_y &= \frac{1}{\sqrt{[R'(\theta)]^2 + R^2(\theta)}} \left(R'(\theta) \sin(\theta) + R(\theta) \cos(\theta), -R'(\theta) \cos(\theta) + R(\theta) \sin(\theta) \right), \\ \text{and } dS_y &= \sqrt{[R'(\theta)]^2 + R^2(\theta)} d\theta. \end{aligned}$$

Using the mean-curvature formula in the 2-dimensional case for $r = R(\theta)$, we also have

$$(3.9) \quad \kappa_R = \frac{R^2 + 2(R')^2 - RR''}{[R^2 + (R')^2]^{\frac{3}{2}}}.$$

For notational convenience, we denote $\kappa_R(\hat{\theta}) = \kappa_R(\mathbf{x})$ and $\kappa_R(\theta) = \kappa_R(\mathbf{y})$. Both $\kappa_R(\hat{\theta})$ and $\kappa_R(\theta)$ can be computed by (3.9).

Based on the above calculations, we rewrite the left-hand side of (3.7) as a functional of $R(\theta)$ as follows

$$(3.10) \quad \begin{aligned} \mathcal{L}[R](\hat{\theta}) \triangleq \int_0^{2\pi} & \left[\beta G_1(D[R]) \sqrt{[R'(\theta)]^2 + R^2(\theta)} - \left((\mu + \kappa_R(\theta)) Q(D[R]) - \frac{\kappa_R(\theta) - \kappa_R(\hat{\theta})}{2\pi(D[R])^2} \right) \right. \\ & \left. \left(R^2(\theta) + R(\hat{\theta})R'(\theta) \sin(\hat{\theta} - \theta) - R(\hat{\theta})R(\theta) \cos(\hat{\theta} - \theta) \right) \right] d\theta, \end{aligned}$$

for $\hat{\theta} \in [0, 2\pi]$. Equation (3.7) implies that $\mathcal{L}[R](\hat{\theta}) \equiv 0$. To regularize the singularity of the kernel, we introduce a small constant $\tau > 0$ in $D[R]$, namely,

$$(3.11) \quad D_\tau[R] = \sqrt{R^2(\hat{\theta}) + R^2(\theta) - 2R(\hat{\theta})R(\theta) \cos(\hat{\theta} - \theta) + \tau^2},$$

and define the corresponding functional for each $\hat{\theta} \in [0, 2\pi]$,

$$(3.12) \quad \begin{aligned} \mathcal{L}_\tau[R](\hat{\theta}) \triangleq \int_0^{2\pi} & \left[\beta G_1(D_\tau[R]) \sqrt{[R'(\theta)]^2 + R^2(\theta)} - \left((\mu + \kappa_R(\theta)) Q(D_\tau[R]) - \frac{\kappa_R(\theta) - \kappa_R(\hat{\theta})}{2\pi(D_\tau[R])^2} \right) \right. \\ & \left. \left(R^2(\theta) + R(\hat{\theta})R'(\theta) \sin(\hat{\theta} - \theta) - R(\hat{\theta})R(\theta) \cos(\hat{\theta} - \theta) \right) \right] d\theta, \end{aligned}$$

Hence we recover (3.10) when $\tau \rightarrow 0$ and have a non-singular kernel when $\tau > 0$. In section 3, we shall prove that (3.12) is a good approximation of (3.10).

Based on machine learning techniques, an approximation of $R(\theta)$ by a single hidden layer neural network is written as

$$(3.13) \quad R(\theta) \approx \sum_{i=1}^N a_i \Psi(b_i \theta + c_i) + d \triangleq \rho(\theta; \mathcal{X}),$$

where N is the width, $\mathcal{X} = (a_1, \dots, a_N, b_1, \dots, b_N, c_1, \dots, c_N, d) \in \mathbb{R}^{3N+1}$ is the neural network's parameter, and Ψ is the nonlinear "activation" function such as sigmoid function. Note that for each ρ , the operator $\mathcal{L}_\tau[\rho](\hat{\theta}_i)$ can be calculated analytically, where $\hat{\theta}_i$ are m randomly sampled points, which are i.i.d. in $[0, 2\pi]$. We consider the loss function:

$$(3.14) \quad F(\mathcal{X}, \hat{\theta}) \triangleq \frac{1}{m} \sum_{i=1}^m \left(\mathcal{L}_\tau[\rho](\hat{\theta}_i) \right)^2 + \sum_{\alpha=0}^2 \left(D^\alpha(\rho(0; \mathcal{X}) - \rho(2\pi; \mathcal{X})) \right)^2.$$

The reason why we choose up to second-order derivative in the second term is that the curvature term involves at most second-order derivative, hence we shall guarantee the continuity up to second-order. The loss function (3.14) measures how well the function $\rho(\theta; \mathcal{X})$ satisfies equation (3.7) as well as the 2π -periodic boundary condition (3.8). Hence \mathcal{X} is obtained via solving the following optimization problem

$$(3.15) \quad \begin{aligned} \min_{\mathcal{X}} J(\mathcal{X}) & \triangleq \mathbb{E}_{\hat{\theta}}[F(\mathcal{X}, \hat{\theta})] = \mathbb{E}_{\hat{\theta}_i} \left[\left(\mathcal{L}_\tau[\rho](\hat{\theta}_i) \right)^2 \right] + \sum_{\alpha=0}^2 \left(D^\alpha \rho(0; \mathcal{X}) - D^\alpha \rho(2\pi; \mathcal{X}) \right)^2 \\ & = \int_0^{2\pi} \left(\mathcal{L}_\tau[\rho](\hat{\theta}_i) \right)^2 \nu(\hat{\theta}_i) d\hat{\theta}_i + \sum_{\alpha=0}^2 \left(D^\alpha \rho(0; \mathcal{X}) - D^\alpha \rho(2\pi; \mathcal{X}) \right)^2, \end{aligned}$$

where $\nu(\hat{\theta}_i)$ is a probability density of $\hat{\theta}_i \in [0, 2\pi]$.

3.3. Stochastic gradient descent training algorithm. In order to solve (3.15) numerically, we use the stochastic gradient descent method shown in Algorithm 1.

Algorithm 1

Choose an initial guess \mathcal{X}_1
for $k = 1, 2, \dots$ **do**
 Generate m random points $\hat{\theta}_k = (\hat{\theta}_{k,i})_{i=1}^m$ from $[0, 2\pi]$;
 Calculate the loss function at randomly sampled points $F(\mathcal{X}_k, \hat{\theta}_k)$;
 Compute a stochastic vector $G(\mathcal{X}_k, \hat{\theta}_k) = \nabla_{\mathcal{X}} F(\mathcal{X}_k, \hat{\theta}_k)$;
 Set the new iterate as $\mathcal{X}_{k+1} = \mathcal{X}_k - \alpha_n G(\mathcal{X}_k, \hat{\theta}_k)$;
end for

Due to the non-convexity of $J(\mathcal{X})$, \mathcal{X}_k may stuck at a local minimum (not a global minimum). Nevertheless, stochastic gradient descent has proven very effective in training deep learning models to obtain the global minimum.

4. CONVERGENCE OF THE NEURAL NETWORK DISCRETIZATION

In this section, we shall prove that the numerical solution with the neural network discretization converges to the unknown boundary of system (2.4) as the number of hidden units tends to infinity, namely,

there exists $\rho \in \mathcal{C}^N$ such that $J(\rho(\theta; \mathcal{X})) \rightarrow 0$ as $n \rightarrow \infty$;

where

$$(4.1) \quad \mathcal{C}^N : \{\rho^N(\theta) : [0, 2\pi] \rightarrow \mathbb{R} \mid \rho^N(\theta) = \sum_{i=1}^N a_i \Psi(b_i \theta + c_i) + d\}.$$

The precise statement is included in Theorem 4.1.

4.1. Preliminary estimates. Denote

$$\begin{aligned} h(\mathbf{x}) &= \int_{\partial\Omega} \beta G_1(D[R]) dS_y, \\ g(\mathbf{x}) &= \int_{\partial\Omega} (\mu + \kappa_R(\mathbf{y})) Q(D[R])(\mathbf{y} - \mathbf{x}) \cdot \mathbf{n}_y dS_y, \\ w(\mathbf{x}) &= \int_{\partial\Omega} \frac{\kappa_R(\mathbf{y}) - \kappa_R(\mathbf{x})}{2\pi} \frac{\mathbf{y} - \mathbf{x}}{(D[R])^2} \cdot \mathbf{n}_y dS_y. \end{aligned}$$

Then the operator \mathcal{L} in (3.10) can be separated into three parts, namely,

$$\mathcal{L}[R](\mathbf{x}) = h(\mathbf{x}) - g(\mathbf{x}) + w(\mathbf{x}).$$

As mentioned before, since $G_1(\mathbf{x}, \mathbf{y}) = G_1(|\mathbf{x} - \mathbf{y}|) = \frac{i}{4} H_0^{(1)}(i|\mathbf{x} - \mathbf{y}|)$ is singular at $|\mathbf{x} - \mathbf{y}| = 0$, we further introduce,

$$\begin{aligned} h_\tau(\mathbf{x}) &= \int_{\partial\Omega} \beta G_1(D_\tau[R]) dS_y, \\ g_\tau(\mathbf{x}) &= \int_{\partial\Omega} (\mu + \kappa_R(\mathbf{y})) Q(D_\tau[R])(\mathbf{y} - \mathbf{x}) \cdot \mathbf{n}_y dS_y, \\ w_\tau(\mathbf{x}) &= \int_{\partial\Omega} \frac{\kappa_R(\mathbf{y}) - \kappa_R(\mathbf{x})}{2\pi} \frac{\mathbf{y} - \mathbf{x}}{(D_\tau[R])^2} \cdot \mathbf{n}_y dS_y. \end{aligned}$$

Correspondingly, \mathcal{L}_τ in (3.12) is also separated into three pieces:

$$\mathcal{L}_\tau[R](\mathbf{x}) = h_\tau(\mathbf{x}) - g_\tau(\mathbf{x}) + w_\tau(\mathbf{x}).$$

By *Lemmas 7.6 – 7.8* in [42], we have the following results:

Lemma 4.1. *Suppose that $\partial\Omega : r = R(\theta) \in C^3(-\infty, \infty)$ and 2π -periodic, then*

$$(4.2) \quad \|h - h_\tau\|_{L^\infty} \leq C\tau |\ln \tau|,$$

$$(4.3) \quad \|g - g_\tau\|_{L^\infty} \leq C\|\kappa_R\|_{C^1}\tau \leq C\tau,$$

$$(4.4) \quad \|w - w_\tau\|_{L^\infty} \leq C\|\kappa_R\|_{C^1}\tau \leq C\tau,$$

where the constant C is independent of τ .

Proof. The proof is really lengthy, here we only point out some key steps. Our definition of $h(\mathbf{x})$ and $h_\tau(\mathbf{x})$ are equivalent to $h(\hat{s})$ and $h_\varepsilon(\hat{s})$ when $f(s) = \beta$ [42, (93)] (Note that functions in [42] are defined based on curve length s . Although they look different from our definitions, they are actually equivalent to our definitions of functions. The curve length parameters s and \hat{s} correspond to the parameters \mathbf{y} and \mathbf{x} here.) Hence (4.2) directly follows from Lemma 7.6. Similarly, $g(\mathbf{x})$ and $g_\tau(\mathbf{x})$ are equivalent to $g(\hat{s})$ and $g_\varepsilon(\hat{s})$ when $f(s) = \mu + \kappa_R(\mathbf{y})$. Combining Lemma 7.7 and 7.8, we shall get estimate (4.3). Finally, for $w(\mathbf{x})$, we use (3.5) to obtain

$$w(\mathbf{x}) = \int_{\partial\Omega} \frac{\kappa_R(\mathbf{y})}{2\pi} \frac{\mathbf{y} - \mathbf{x}}{(D[R])^2} \cdot \mathbf{n}_y dS_y - \frac{\kappa_R(\mathbf{x})}{2} \triangleq w_1(\mathbf{x}) - \frac{\kappa_R(\mathbf{x})}{2},$$

hence $w_1(\mathbf{x}) = w(\mathbf{x}) + \frac{\kappa_R(\mathbf{x})}{2} = \int_{\partial\Omega} \frac{\kappa_R(\mathbf{y})}{2\pi} \frac{\mathbf{y} - \mathbf{x}}{(D[R])^2} \cdot \mathbf{n}_y dS_y$. On the other hand, we denote

$$w_{1\tau}(\mathbf{x}) = w_\tau(\mathbf{x}) + \frac{\kappa_R(\mathbf{x})}{2} = \frac{\kappa_R(\mathbf{x})}{2} + \int_{\partial\Omega} \frac{\kappa_R(\mathbf{y}) - \kappa_R(\mathbf{x})}{2\pi} \frac{\mathbf{y} - \mathbf{x}}{(D_\tau[R])^2} \cdot \mathbf{n}_y dS_y.$$

In this way, $w_1(\mathbf{x})$ and $w_{1\tau}(\mathbf{x})$ are equivalent to $-g_1(\hat{s})$ and $-g_{1\varepsilon}(\hat{s})$ when $f(s) = \kappa_R(\mathbf{y})$ and $f(\hat{s}) = \kappa_R(\mathbf{x})$ [42, (110), (111)]. According to

$$([14, (112)]) \quad \|g_1 - g_{1\varepsilon}\|_{L^\infty} \leq C\|f\|_{C^1}\varepsilon,$$

estimate (4.4) can be derived. Notice that we need $\|\kappa_R\|_{C^1}$ in both (4.3) and (4.4), and κ_R involves at most second-order derivative of $R(\theta)$, hence we require $\partial\Omega : r = R(\theta) \in C^3$. \square

Based on Lemma 4.1, we shall have

$$\|(\mathcal{L}_\tau - \mathcal{L})[R]\|_{L^\infty} \leq \|h - h_\tau\|_{L^\infty} + \|g - g_\tau\|_{L^\infty} + \|w - w_\tau\|_{L^\infty} \leq C\tau |\ln \tau| + C\tau,$$

which indicates that (3.12) is a good approximation of (3.10). Recall that it follows from (3.7) that $\mathcal{L}[R] \equiv 0$, then we immediately derive

$$(4.5) \quad \|\mathcal{L}_\tau[R]\|_{L^\infty} \leq C\tau |\ln \tau| + C\tau.$$

4.2. The neural network approximation. By Theorem 3 of [43] we know that if the activation function $\Psi \in C^3(\mathbb{R})$ is nonconstant and bounded, then the space $\cup_{n=1}^\infty \mathcal{C}^n$ is uniformly 3-dense on compacta in $C^3(\mathbb{R})$. This means that for $R(\theta) \in C^3(-\infty, \infty)$ and every $0 < \delta < 1$, there is $\rho(\theta; \mathcal{X}) \in \cup_{N=1}^\infty \mathcal{C}^N$ such that

$$(4.6) \quad \|\rho - R\|_{3, [0, 2\pi]} \leq \delta,$$

where $\|f\|_{3, [0, 2\pi]} := \max_{\alpha \leq 3} \sup_{x \in [0, 2\pi]} |D^\alpha f(x)|$. Clearly, (4.7) implies

$$(4.7) \quad \|\rho - R\|_{L^\infty([0, 2\pi])}, \|\rho' - R'\|_{L^\infty([0, 2\pi])}, \|\rho'' - R''\|_{L^\infty([0, 2\pi])}, \|\rho''' - R'''\|_{L^\infty([0, 2\pi])} \leq \delta.$$

Based on (4.7), let's first bound $\|\mathcal{L}_\tau[\rho - R]\|_{L^\infty}$, which is a key estimate in proving the convergence theorem. Throughout the rest of this paper, C is used to represent a generic constant independent of τ and δ , which might change from a line to next.

Recall the formulas for $\mathcal{L}_\tau[R]$ and $D_\tau[R]$ in (3.12) and (3.11), respectively:

$$\begin{aligned} \mathcal{L}_\tau[R](\hat{\theta}) = \int_0^{2\pi} \left[\beta G_1(D_\tau[R]) \sqrt{[R'(\theta)]^2 + R^2(\theta)} - \left((\mu + \kappa_R(\theta)) Q(D_\tau[R]) - \frac{\kappa_R(\theta) - \kappa_R(\hat{\theta})}{2\pi(D_\tau[R])^2} \right) \right. \\ \left. \left(R^2(\theta) + R(\hat{\theta})R'(\theta) \sin(\hat{\theta} - \theta) - R(\hat{\theta})R(\theta) \cos(\hat{\theta} - \theta) \right) \right] d\theta, \end{aligned}$$

$$D_\tau[R] = \sqrt{R^2(\hat{\theta}) + R^2(\theta) - 2R(\hat{\theta})R(\theta) \cos(\hat{\theta} - \theta) + \tau^2}.$$

Correspondingly, $\mathcal{L}_\tau[\rho]$ takes the following form

$$(4.8) \quad \mathcal{L}_\tau[\rho](\hat{\theta}) = \int_0^{2\pi} \left[\beta G_1(D_\tau[\rho]) \sqrt{[\rho'(\theta)]^2 + \rho^2(\theta)} - \left((\mu + \kappa_\rho(\theta)) Q(D_\tau[\rho]) - \frac{\kappa_\rho(\theta) - \kappa_\rho(\hat{\theta})}{2\pi(D_\tau[\rho])^2} \right) \right. \\ \left. \left(\rho^2(\theta) + \rho(\hat{\theta})\rho'(\theta) \sin(\hat{\theta} - \theta) - \rho(\hat{\theta})\rho(\theta) \cos(\hat{\theta} - \theta) \right) \right] d\theta,$$

where

$$(4.9) \quad D_\tau[\rho] = \sqrt{\rho^2(\hat{\theta}) + \rho^2(\theta) - 2\rho(\hat{\theta})\rho(\theta) \cos(\hat{\theta} - \theta) + \tau^2}.$$

Notice that we use κ_R and κ_ρ to differentiate the curvature on different curves. By (3.9),

$$(4.10) \quad \kappa_R = \frac{R^2 + 2(R')^2 - RR''}{[R^2 + (R')^2]^{\frac{3}{2}}}, \quad \text{and} \quad \kappa_\rho = \frac{\rho^2 + 2(\rho')^2 - \rho\rho''}{[\rho^2 + (\rho')^2]^{\frac{3}{2}}}.$$

Subtracting $\mathcal{L}_\tau[\rho]$ from $\mathcal{L}_\tau[R]$, we derive, for each $\hat{\theta} \in [0, 2\pi]$,

$$\begin{aligned} |\mathcal{L}_\tau[\rho - R](\hat{\theta})| &\leq \beta \int_0^{2\pi} \left| G_1(D_\tau[\rho]) \sqrt{[\rho'(\theta)]^2 + \rho^2(\theta)} - G_1(D_\tau[R]) \sqrt{[R'(\theta)]^2 + R^2(\theta)} \right| d\theta \\ &\quad + \int_0^{2\pi} \left| Q(D_\tau[\rho]) \left(\mu + \kappa_\rho(\theta) \right) \left(\rho^2(\theta) + \rho(\hat{\theta})\rho'(\theta) \sin(\hat{\theta} - \theta) - \rho(\hat{\theta})\rho(\theta) \cos(\hat{\theta} - \theta) \right) \right. \\ &\quad \left. - Q(D_\tau[R]) \left(\mu + \kappa_R(\theta) \right) \left(R^2(\theta) + R(\hat{\theta})R'(\theta) \sin(\hat{\theta} - \theta) - R(\hat{\theta})R(\theta) \cos(\hat{\theta} - \theta) \right) \right| d\theta \\ &\quad + \int_0^{2\pi} \left| \frac{\kappa_\rho(\theta) - \kappa_\rho(\hat{\theta})}{2\pi(D_\tau[\rho])^2} \left(\rho^2(\theta) + \rho(\hat{\theta})\rho'(\theta) \sin(\hat{\theta} - \theta) - \rho(\hat{\theta})\rho(\theta) \cos(\hat{\theta} - \theta) \right) \right. \\ &\quad \left. - \frac{\kappa_R(\theta) - \kappa_R(\hat{\theta})}{2\pi(D_\tau[R])^2} \left(R^2(\theta) + R(\hat{\theta})R'(\theta) \sin(\hat{\theta} - \theta) - R(\hat{\theta})R(\theta) \cos(\hat{\theta} - \theta) \right) \right| d\theta \\ &\triangleq \beta \int_0^{2\pi} |\text{I}| d\theta + \int_0^{2\pi} |\text{II}| d\theta + \int_0^{2\pi} |\text{III}| d\theta. \end{aligned}$$

In order to estimate $|\mathcal{L}_\tau[\rho - R](\hat{\theta})|$, we need to estimate $|\text{I}|$, $|\text{II}|$, and $|\text{III}|$, respectively. For term I, we insert a term $G_1(D_\tau[\rho]) \sqrt{[R'(\theta)]^2 + R^2(\theta)}$ and subtract the same term; after rearranging the terms in I, we obtain

$$(4.11) \quad |\text{I}| \leq \left| G_1(D_\tau[\rho]) \right| \left| \sqrt{[\rho'(\theta)]^2 + \rho^2(\theta)} - \sqrt{[R'(\theta)]^2 + R^2(\theta)} \right| \\ + \left| G_1(D_\tau[\rho]) - G_1(D_\tau[R]) \right| \sqrt{[R'(\theta)]^2 + R^2(\theta)}.$$

Using the inequality $|\sqrt{x} - \sqrt{y}| \leq \sqrt{|x - y|}$, and combining with estimates (4.7), we have

$$(4.12) \quad \begin{aligned} \left| \sqrt{[\rho'(\theta)]^2 + \rho^2(\theta)} - \sqrt{[R'(\theta)]^2 + R^2(\theta)} \right| &\leq \sqrt{[\rho'(\theta)]^2 + \rho^2(\theta) - [R'(\theta)]^2 - R^2(\theta)} \\ &\leq \sqrt{[\rho'(\theta)]^2 - [R'(\theta)]^2} + \sqrt{|\rho^2(\theta) - R^2(\theta)|} \\ &\leq C\delta^{\frac{1}{2}}. \end{aligned}$$

In a similar manner, $|D_\tau[\rho] - D_\tau[R]|$ can also be estimated:

$$(4.13) \quad \begin{aligned} |D_\tau[\rho] - D_\tau[R]| &\leq \sqrt{\left| \rho^2(\hat{\theta}) + \rho^2(\theta) - R^2(\hat{\theta}) - R^2(\theta) - 2(\rho(\hat{\theta})\rho(\theta) - R(\hat{\theta})R(\theta)) \cos(\hat{\theta} - \theta) \right|} \\ &\leq \sqrt{\left| \rho^2(\hat{\theta}) - R^2(\hat{\theta}) \right| + \left| \rho^2(\theta) - R^2(\theta) \right| + 2\left| \rho(\hat{\theta})\rho(\theta) - R(\hat{\theta})R(\theta) \right|} \\ &\leq C\delta^{\frac{1}{2}}. \end{aligned}$$

In addition, since $R \in C^2$, we clearly have

$$(4.14) \quad \sqrt{[R'(\theta)]^2 + R^2(\theta)} \leq C.$$

Next we proceed to consider the terms involving G_1 . We compute

$$G_1(r) = \frac{i}{4}H_0^{(1)}(ir), \quad \text{and} \quad G_1'(r) = -\frac{1}{4}(H_0^{(1)})'(ir) = \frac{1}{4}H_1^{(1)}(ir);$$

and it is clear that both $G_1(r)$ and $G_1'(r)$ are singular at $r = 0$. Here we collect some formulas for the Hankel function, and we focus on the approximation when $r \rightarrow 0$:

$$\begin{aligned} H_0^{(1)}(z) &= J_0(z) + iY_0(z), & H_1^{(1)}(z) &= J_1(z) + iY_1(z), & ([9.1.3] \text{ of } [44]), \\ J_0(z) &= \phi_1(-z^2), & \phi_1(0) &= 1, & \phi_1 \in C^\infty, & ([9.1.12] \text{ of } [44]), \\ Y_0(z) &= \frac{2}{\pi} \left[\ln\left(\frac{1}{2}z\right) + \gamma \right] J_0(z) + \phi_2(z^2), & \phi_2 \in C^\infty, & ([9.1.13] \text{ of } [44]), \\ J_1(z) &= \frac{1}{2}z\phi_3(-z^2), & \phi_3(0) &= 1, & \phi_3 \in C^\infty, & ([9.1.10] \text{ of } [44]), \\ Y_1(z) &= -\frac{2}{\pi z} + \frac{2}{\pi} \ln\left(\frac{1}{2}z\right) J_1(z) - \frac{z}{2\pi} \phi_4(-z^2), & \phi_4 \in C^\infty, & ([9.1.11] \text{ of } [44]). \end{aligned}$$

It follows that

$$\begin{aligned} G_1(r) &= \frac{i}{4}H_0^{(1)}(ir) = -\frac{1}{2\pi} \ln r \cdot \phi_1(r^2) + \phi_5(r^2), & \phi_5 \in C^\infty; \\ G_1'(r) &= \frac{1}{4}H_1^{(1)}(ir) = -\frac{1}{2\pi r} - \frac{1}{4\pi} r \ln r \cdot \phi_3(r^2) + r\phi_6(r^2), & \phi_6 \in C^\infty. \end{aligned}$$

Since $\tau > 0$, both $D_\tau[\rho]$ and $D_\tau[R]$ are greater than τ ; hence there exists a constant C which is independent of τ and δ such that

$$\begin{aligned} |G_1(D_\tau[\rho])| &\leq C|\ln \tau| \\ |G_1(D_\tau[\rho]) - G_1(D_\tau[R])| &\leq \frac{C}{\tau} |D_\tau[\rho] - D_\tau[R]|. \end{aligned}$$

Substituting the above two inequalities, and estimates (4.12), (4.13) as well as (4.14) all into (4.11), we finally derive

$$(4.15) \quad |I| \leq C|\ln \tau| \delta^{\frac{1}{2}} + \frac{C}{\tau} \delta^{\frac{1}{2}},$$

where the constant C is independent of τ and δ .

After we show the bound for I, we can estimate II and III in the same manner. Recall that

$$Q(r) = \frac{1}{r} \left(G_1'(r) + \frac{1}{2\pi r} \right),$$

then

$$Q(r) = -\frac{1}{4\pi} \ln r \cdot \phi_3(r^2) + \phi_6(r^2), \quad Q'(r) = O(r^{-1}).$$

Therefore, similar as function G_1 , there exists a constant C not independent of τ and δ such that

$$\begin{aligned} |Q(D_\tau[\rho])| &\leq C|\ln \tau| \\ |Q(D_\tau[\rho]) - Q(D_\tau[R])| &\leq \frac{C}{\tau} |D_\tau[\rho] - D_\tau[R]|. \end{aligned}$$

Next we turn our attention to the terms involving the curvature. Since $R, \rho \in C^3$, κ_R and κ_ρ are both bounded based on (4.10) (note that we are only interested in the solutions which are away from the origin, hence the denominator of the curvature is not close to 0). Moreover, subtracting κ_ρ from κ_R , recalling also (4.12) and (4.7), we have

$$\begin{aligned} |\kappa_\rho - \kappa_R| &\leq \left| \frac{\rho^2 + 2(\rho')^2 - \rho\rho''}{[\rho^2 + (\rho')^2]^{\frac{3}{2}}} - \frac{\rho^2 + 2(\rho')^2 - \rho\rho''}{[R^2 + (R')^2]^{\frac{3}{2}}} \right| + \left| \frac{\rho^2 + 2(\rho')^2 - \rho\rho''}{[R^2 + (R')^2]^{\frac{3}{2}}} - \frac{R^2 + 2(R')^2 - RR''}{[R^2 + (R')^2]^{\frac{3}{2}}} \right| \\ &\leq C \left| (\sqrt{\rho^2 + (\rho')^2})^3 - (\sqrt{R^2 + (R')^2})^3 \right| + C \left| \rho^2 - R^2 + 2(\rho')^2 - 2(R')^2 - \rho\rho'' + RR'' \right| \\ &\leq C \left| \sqrt{\rho^2 + (\rho')^2} - \sqrt{R^2 + (R')^2} \right| + C\delta \\ &\leq C\delta^{\frac{1}{2}} + C\delta \leq C\delta^{\frac{1}{2}} \end{aligned}$$

Therefore, we derive

$$\begin{aligned}
(4.16) \quad |\text{II}| &\leq \left| Q(D_\tau[\rho]) \right| \left| \mu + \kappa_\rho \right| \left| \rho^2(\theta) - R^2(\theta) + (\rho(\hat{\theta})\rho'(\theta) - R(\hat{\theta})R'(\theta)) \sin(\hat{\theta} - \theta) \right. \\
&\quad \left. - (\rho(\hat{\theta})\rho(\theta) - R(\hat{\theta})R(\theta)) \cos(\hat{\theta} - \theta) \right| \\
&\quad + \left| Q(D_\tau[\rho]) \right| \left| \kappa_\rho - \kappa_R \right| \left| R^2(\theta) + R(\hat{\theta})R'(\theta) \sin(\hat{\theta} - \theta) - R(\hat{\theta})R(\theta) \cos(\hat{\theta} - \theta) \right| \\
&\quad + \left| Q(D_\tau[\rho]) - Q(D_\tau[R]) \right| \left| \mu + \kappa_R \right| \left| R^2(\theta) + R(\hat{\theta})R'(\theta) \sin(\hat{\theta} - \theta) - R(\hat{\theta})R(\theta) \cos(\hat{\theta} - \theta) \right| \\
&\leq C |\ln \tau| \delta + C |\ln \tau| \delta^{\frac{1}{2}} + \frac{C}{\tau} \delta^{\frac{1}{2}} \leq C |\ln \tau| \delta^{\frac{1}{2}} + \frac{C}{\tau} \delta^{\frac{1}{2}}
\end{aligned}$$

$$\begin{aligned}
(4.17) \quad |\text{III}| &\leq \left| \frac{\kappa_\rho(\theta) - \kappa_\rho(\hat{\theta})}{2\pi(D_\tau[\rho])^2} \right| \left| \rho^2(\theta) - R^2(\theta) + (\rho(\hat{\theta})\rho'(\theta) - R(\hat{\theta})R'(\theta)) \sin(\hat{\theta} - \theta) \right. \\
&\quad \left. - (\rho(\hat{\theta})\rho(\theta) - R(\hat{\theta})R(\theta)) \cos(\hat{\theta} - \theta) \right| \\
&\quad + \left| \frac{\kappa_\rho(\theta) - \kappa_\rho(\hat{\theta})}{2\pi(D_\tau[\rho])^2} - \frac{\kappa_\rho(\theta) - \kappa_\rho(\hat{\theta})}{2\pi(D_\tau[R])^2} \right| \left| R^2(\theta) + R(\hat{\theta})R'(\theta) \sin(\hat{\theta} - \theta) - R(\hat{\theta})R(\theta) \cos(\hat{\theta} - \theta) \right| \\
&\quad + \left| \frac{\kappa_\rho(\theta) - \kappa_R(\theta) - \kappa_\rho(\hat{\theta}) + \kappa_R(\hat{\theta})}{2\pi(D_\tau[R])^2} \right| \left| R^2(\theta) + R(\hat{\theta})R'(\theta) \sin(\hat{\theta} - \theta) - R(\hat{\theta})R(\theta) \cos(\hat{\theta} - \theta) \right| \\
&\leq \frac{C}{\tau^2} \delta + \frac{C}{\tau^3} \delta^{\frac{1}{2}} + \frac{C}{\tau^2} \delta^{\frac{1}{2}} \leq \frac{C}{\tau^3} \delta^{\frac{1}{2}}
\end{aligned}$$

Now we are able to estimate $|\mathcal{L}_\tau[\rho - R](\hat{\theta})|$. Recall that

$$|\mathcal{L}_\tau[\rho - R](\hat{\theta})| \leq \beta \int_0^{2\pi} |\text{I}| d\theta + \int_0^{2\pi} |\text{II}| d\theta + \int_0^{2\pi} |\text{III}| d\theta;$$

together with (4.15), (4.16) and (4.17), it follows that, for each $\hat{\theta} \in [0, 2\pi]$,

$$\begin{aligned}
|\mathcal{L}_\tau[\rho - R](\hat{\theta})| &\leq 2\beta\pi \max |\text{I}| + 2\pi \max |\text{II}| + 2\pi \max |\text{III}| \\
&\leq 2\beta\pi \left(C |\ln \tau| \delta^{\frac{1}{2}} + \frac{C}{\tau} \delta^{\frac{1}{2}} \right) + 2\pi \left(C |\ln \tau| \delta^{\frac{1}{2}} + \frac{C}{\tau} \delta^{\frac{1}{2}} \right) + 2\pi \frac{C}{\tau^3} \delta^{\frac{1}{2}} \\
&\leq C |\ln \tau| \delta^{\frac{1}{2}} + \frac{C}{\tau^3} \delta^{\frac{1}{2}},
\end{aligned}$$

which is equivalent to

$$(4.18) \quad \|\mathcal{L}_\tau[\rho - R]\|_{L^\infty} \leq C |\ln \tau| \delta^{\frac{1}{2}} + \frac{C}{\tau^3} \delta^{\frac{1}{2}}.$$

4.3. Convergence theorem. Here is our convergence theorem:

Theorem 4.1. *Let $\mathcal{C}^n(\Psi)$ be given by (4.1) where Ψ is assumed to be in $C^3(\mathbb{R})$, bounded and non-constant. Then for every $0 < \delta < 1$, there exists $\rho(\theta; \mathcal{X}) \in \cup_{N=1}^\infty \mathcal{C}^N$ and a positive constant K such that*

$$J(\rho(\theta; \mathcal{X})) \leq K \delta^{\frac{1}{8}},$$

where the constant K does not depend upon δ .

Proof. We start from the definition of J in (3.15). Notice that R satisfies the 2π -periodic boundary condition, i.e., $R(0) = R(2\pi)$, $R'(0) = R'(2\pi)$, $R''(0) = R''(2\pi)$. Therefore, we have

$$\begin{aligned}
J(\rho(\theta; \mathcal{X})) &= \int_0^{2\pi} (\mathcal{L}_\tau[\rho](\hat{\theta}_i))^2 \nu(\hat{\theta}_i) d\hat{\theta}_i + \sum_{\alpha=0}^2 \left(D^\alpha(\rho(0; \mathcal{X}) - \rho(2\pi; \mathcal{X})) \right)^2 \\
&= \int_0^{2\pi} (\mathcal{L}_\tau[\rho - R](\hat{\theta}_i) + \mathcal{L}_\tau[R](\hat{\theta}_i))^2 \nu(\hat{\theta}_i) d\hat{\theta}_i + \sum_{\alpha=0}^2 \left(D^\alpha(\rho(0; \mathcal{X}) - R(0) - \rho(2\pi; \mathcal{X}) + R(2\pi)) \right)^2 \\
&\leq 2 \int_0^{2\pi} (\mathcal{L}_\tau[\rho - R](\hat{\theta}_i))^2 \nu(\hat{\theta}_i) d\hat{\theta}_i + 2 \int_0^{2\pi} (\mathcal{L}_\tau[R](\hat{\theta}_i))^2 \nu(\hat{\theta}_i) d\hat{\theta}_i \\
&\quad + 2 \sum_{\alpha=0}^2 \left((\rho(0; \mathcal{X}) - R(0)) \right)^2 + 2 \sum_{\alpha=0}^2 \left((\rho(2\pi; \mathcal{X}) - R(2\pi)) \right)^2 \\
&\leq 2 \|\mathcal{L}_\tau[\rho - R]\|_{L^\infty}^2 + 2 \|\mathcal{L}_\tau[R]\|_{L^\infty}^2 + 12 \|\rho - R\|_{2, [0, 2\pi]}^2.
\end{aligned}$$

We combine it with estimates in (4.5), (4.7) as well as (4.18), and use the fact that $(a+b)^2 \leq 2(a^2 + b^2)$, to obtain

$$J(\rho(\theta; \mathcal{X})) \leq C \left(|\ln \tau|^2 \delta + \frac{\delta}{\tau^6} + |\ln \tau|^2 \tau^2 + \tau^2 + \delta^2 \right).$$

Take $\tau = \delta^{\frac{1}{8}}$, we have

$$J(\rho(\theta; \mathcal{X})) \leq C \left(|\ln \delta^{\frac{1}{8}}|^2 \delta + \delta^{\frac{1}{4}} + |\ln \delta^{\frac{1}{8}}|^2 \delta^{\frac{1}{4}} + \delta^{\frac{1}{4}} + \delta^2 \right) \leq C \left(|\ln \delta^{\frac{1}{8}}|^2 \delta^{\frac{1}{4}} + \delta^{\frac{1}{4}} \right).$$

It is easy to show, for $0 < x < 1$,

$$|\ln x|^2 x^2 < x;$$

hence when $0 < \delta < 1$,

$$|\ln \delta^{\frac{1}{8}}|^2 \delta^{\frac{1}{4}} \leq \delta^{\frac{1}{8}}.$$

By choosing $K = 2C$, we finally obtain

$$J(f) \leq C \left(\delta^{\frac{1}{8}} + \delta^{\frac{1}{4}} \right) \leq 2C \delta^{\frac{1}{8}} \leq K \delta^{\frac{1}{8}}$$

which completes the proof. \square

5. CONVERGENCE FOR THE STOCHASTIC GRADIENT DESCENT

In this section, we will prove the convergence of the stochastic gradient descent. Recall the loss function we consider in (3.14),

$$(5.1) \quad F(\mathcal{X}, \hat{\theta}) = \frac{1}{m} \sum_{i=1}^m \left(\mathcal{L}_\tau[\rho](\hat{\theta}_i) \right)^2 + \sum_{\alpha=0}^2 \left(D^\alpha \rho(0; \mathcal{X}) - D^\alpha \rho(2\pi; \mathcal{X}) \right)^2,$$

and

$$(5.2) \quad J(\mathcal{X}) = \mathbb{E}_{\hat{\theta}}[F(\mathcal{X}, \hat{\theta})],$$

$$(5.3) \quad G(\mathcal{X}, \hat{\theta}) = \nabla_{\mathcal{X}} F(\mathcal{X}, \hat{\theta}).$$

We have the following convergence result for the stochastic gradient descent:

Theorem 5.1. *Assume further the activation function Ψ is $C^4(\mathbb{R})$, and $\{\mathcal{X}_k\}$ is contained in a bounded open set, let the stochastic gradient descent method (Algorithm 1) run with a stepsize sequence satisfying*

$$\sum_{k=1}^{\infty} \alpha_k = \infty \quad \text{and} \quad \sum_{k=1}^{\infty} \alpha_k^2 < \infty,$$

then, with $A_k := \sum_{k=1}^K \alpha_k$, the following convergence is obtained,

$$\mathbb{E} \left[\frac{1}{A_k} \sum_{k=1}^K \alpha_k \|\nabla F(\mathcal{X})\|_2^2 \right] \rightarrow 0 \quad \text{as } K \rightarrow \infty.$$

Proof. To proof Theorem 5.1, it suffices to verify the assumptions 4.1 and 4.3 in [45]:

5.1. Lipschitz-continuous objective gradients. First, let's prove that the objective function $J(\mathcal{X})$ is continuously differentiable and the gradient function of J , namely, $\nabla_{\mathcal{X}} J$ is Lipschitz continuous (cf., [45]). Since

$$(5.4) \quad \nabla_{\mathcal{X}} J(\mathcal{X}) = \nabla_{\mathcal{X}} \mathbb{E}_{\hat{\theta}}[F(\mathcal{X}, \hat{\theta})] = \mathbb{E}_{\hat{\theta}}[\nabla_{\mathcal{X}} F(\mathcal{X}, \hat{\theta})],$$

we find that $\nabla_{\mathcal{X}} J$ is Lipschitz continuous if $\nabla_{\mathcal{X}} F(\mathcal{X}, \hat{\theta})$ is bounded and Lipschitz continuous. Therefore, it suffices to derive the regularity of $\nabla_{\mathcal{X}} F(\mathcal{X}, \hat{\theta})$.

Using the definition of $F(\mathcal{X}, \hat{\theta})$ in (5.1), we have

$$\begin{aligned} \nabla_{\mathcal{X}} F(\mathcal{X}, \hat{\theta}) &= \frac{2}{m} \sum_{i=1}^m (\mathcal{L}_{\tau}[\rho](\hat{\theta}_i)) \nabla_{\mathcal{X}} \mathcal{L}_{\tau}[\rho](\hat{\theta}_i) \\ &\quad + 2 \sum_{\alpha=0}^2 (D^{\alpha} \rho(0; \mathcal{X}) - D^{\alpha} \rho(2\pi; \mathcal{X})) \cdot \nabla_{\mathcal{X}} (D^{\alpha} \rho(0; \mathcal{X}) - D^{\alpha} \rho(2\pi; \mathcal{X})), \end{aligned}$$

where $\mathcal{L}_{\tau}[\rho](\hat{\theta}_i)$ is defined in (4.8). For brevity, we denote the integrand in $\mathcal{L}_{\tau}[\rho](\hat{\theta}_i)$ to be function M , namely,

$$\begin{aligned} (5.5) \quad M(\theta, \hat{\theta}_i) &= M(\rho(\theta), \rho(\hat{\theta}_i), \rho'(\theta), \rho'(\hat{\theta}_i), \rho''(\theta), \rho''(\hat{\theta}_i)) \\ &= \beta G_1(D_{\tau}[\rho]) \sqrt{[\rho'(\theta)]^2 + \rho^2(\theta)} - \left((\mu + \kappa_{\rho}(\theta)) Q(D_{\tau}[\rho]) - \frac{\kappa_{\rho}(\theta) - \kappa_{\rho}(\hat{\theta}_i)}{2\pi(D_{\tau}[\rho])^2} \right) \\ &\quad \cdot \left(\rho^2(\theta) + \rho(\hat{\theta}_i) \rho'(\theta) \sin(\hat{\theta}_i - \theta) - \rho(\hat{\theta}_i) \rho(\theta) \cos(\hat{\theta}_i - \theta) \right). \end{aligned}$$

We notice that the function M involves ρ , ρ' , as well as ρ'' . In our settings,

$$(5.6) \quad \rho(\theta) = \sum a_i \Psi(b_i \theta + c_i) + d,$$

hence

$$(5.7) \quad \rho'(\theta) = \sum a_i b_i \Psi'(b_i \theta + c_i),$$

$$(5.8) \quad \rho''(\theta) = \sum a_i b_i^2 \Psi''(b_i \theta + c_i).$$

Clearly, for each $\hat{\theta}_i$,

$$(5.9) \quad \nabla_{\mathcal{X}} \mathcal{L}_{\tau}[\rho](\hat{\theta}_i) = \int_0^{2\pi} \nabla_{\mathcal{X}} M(\theta, \hat{\theta}_i) d\theta,$$

and, by the chain rules,

$$\begin{aligned} (5.10) \quad \nabla_{\mathcal{X}} M &= \frac{\partial M}{\partial \rho(\theta)} \nabla_{\mathcal{X}} \rho(\theta) + \frac{\partial M}{\partial \rho'(\theta)} \nabla_{\mathcal{X}} \rho'(\theta) + \frac{\partial M}{\partial \rho''(\theta)} \nabla_{\mathcal{X}} \rho''(\theta) \\ &\quad + \frac{\partial M}{\partial \rho(\hat{\theta}_i)} \nabla_{\mathcal{X}} \rho(\hat{\theta}_i) + \frac{\partial M}{\partial \rho'(\hat{\theta}_i)} \nabla_{\mathcal{X}} \rho'(\hat{\theta}_i) + \frac{\partial M}{\partial \rho''(\hat{\theta}_i)} \nabla_{\mathcal{X}} \rho''(\hat{\theta}_i) \end{aligned}$$

Let's then deal with each term in (5.10). It follows from (5.5) that

$$\begin{aligned}
\frac{\partial M}{\partial \rho(\theta)} &= \beta G'_1(D_\tau[\rho]) \frac{\partial D_\tau[\rho]}{\partial \rho(\theta)} \sqrt{[\rho'(\theta)]^2 + \rho^2(\theta)} + \beta G_1(D_\tau[\rho]) \frac{\rho(\theta)}{\sqrt{[\rho'(\theta)]^2 + \rho^2(\theta)}} - \left((\mu + \kappa_\rho(\theta)) Q'(D_\tau[\rho]) \right. \\
&\quad \left. + \frac{\kappa_\rho(\theta) - \kappa_\rho(\hat{\theta}_i)}{\pi(D_\tau[\rho])^3} \right) \frac{\partial D_\tau[\rho]}{\partial \rho(\theta)} \left(\rho^2(\theta) + \rho(\hat{\theta}_i) \rho'(\theta) \sin(\hat{\theta}_i - \theta) - \rho(\hat{\theta}_i) \rho(\theta) \cos(\hat{\theta}_i - \theta) \right) - \left(Q(D_\tau[\rho]) \right. \\
&\quad \left. - \frac{1}{2\pi(D_\tau[\rho])^2} \right) \frac{\partial \kappa_\rho(\theta)}{\partial \rho(\theta)} \left(\rho^2(\theta) + \rho(\hat{\theta}_i) \rho'(\theta) \sin(\hat{\theta}_i - \theta) - \rho(\hat{\theta}_i) \rho(\theta) \cos(\hat{\theta}_i - \theta) \right) - \left(Q(D_\tau[\rho]) (\mu \right. \\
&\quad \left. + \kappa_\rho(\theta)) - \frac{\kappa_\rho(\theta) - \kappa_\rho(\hat{\theta}_i)}{2\pi(D_\tau[\rho])^2} \right) \left(2\rho(\theta) - \rho(\hat{\theta}_i) \cos(\hat{\theta}_i - \theta) \right), \\
\frac{\partial M}{\partial \rho(\hat{\theta}_i)} &= \beta G'_1(D_\tau[\rho]) \frac{\partial D_\tau[\rho]}{\partial \rho(\hat{\theta}_i)} \sqrt{[\rho'(\theta)]^2 + \rho^2(\theta)} - \left((\mu + \kappa_\rho(\theta)) Q'(D_\tau[\rho]) + \frac{\kappa_\rho(\theta) - \kappa_\rho(\hat{\theta}_i)}{\pi(D_\tau[\rho])^3} \right) \frac{\partial D_\tau[\rho]}{\partial \rho(\hat{\theta}_i)} \left(\rho^2(\theta) \right. \\
&\quad \left. + \rho(\hat{\theta}_i) \rho'(\theta) \sin(\hat{\theta}_i - \theta) - \rho(\hat{\theta}_i) \rho(\theta) \cos(\hat{\theta}_i - \theta) \right) - \frac{1}{2\pi(D_\tau[\rho])^2} \frac{\partial \kappa_\rho(\hat{\theta}_i)}{\partial \rho(\hat{\theta}_i)} \left(\rho(\hat{\theta}_i) \rho'(\theta) \sin(\hat{\theta}_i - \theta) \right. \\
&\quad \left. + \rho^2(\theta) - \rho(\hat{\theta}_i) \rho(\theta) \cos(\hat{\theta}_i - \theta) \right) - \left((\mu + \kappa_\rho(\theta)) Q(D_\tau[\rho]) - \frac{\kappa_\rho(\theta) - \kappa_\rho(\hat{\theta}_i)}{2\pi(D_\tau[\rho])^2} \right) \left(\rho'(\theta) \sin(\hat{\theta}_i - \theta) \right. \\
&\quad \left. - \rho(\theta) \cos(\hat{\theta}_i - \theta) \right), \\
\frac{\partial M}{\partial \rho'(\theta)} &= \beta G_1(D_\tau[\rho]) \frac{\rho'(\theta)}{\sqrt{[\rho'(\theta)]^2 + \rho^2(\theta)}} - \frac{\partial \kappa_\rho(\theta)}{\partial \rho'(\theta)} \left(Q(D_\tau[\rho]) - \frac{1}{2\pi(D_\tau[\rho])^2} \right) \left(\rho^2(\theta) + \rho(\hat{\theta}_i) \rho'(\theta) \sin(\hat{\theta}_i - \theta) \right. \\
&\quad \left. - \rho(\hat{\theta}_i) \rho(\theta) \cos(\hat{\theta}_i - \theta) \right) - \left((\mu + \kappa_\rho(\theta)) Q(D_\tau[\rho]) - \frac{\kappa_\rho(\theta) - \kappa_\rho(\hat{\theta}_i)}{2\pi(D_\tau[\rho])^2} \right) \rho(\hat{\theta}_i) \sin(\hat{\theta}_i - \theta), \\
\frac{\partial M}{\partial \rho'(\hat{\theta}_i)} &= -\frac{1}{2\pi(D_\tau[\rho])^2} \frac{\partial \kappa_\rho(\hat{\theta}_i)}{\partial \rho'(\hat{\theta}_i)} \left(\rho^2(\theta) + \rho(\hat{\theta}_i) \rho'(\theta) \sin(\hat{\theta}_i - \theta) - \rho(\hat{\theta}_i) \rho(\theta) \cos(\hat{\theta}_i - \theta) \right), \\
\frac{\partial M}{\partial \rho''(\theta)} &= -\frac{\partial \kappa_\rho(\theta)}{\partial \rho''(\theta)} \left(Q(D_\tau[\rho]) - \frac{1}{2\pi(D_\tau[\rho])^2} \right) \left(\rho^2(\theta) + \rho(\hat{\theta}_i) \rho'(\theta) \sin(\hat{\theta}_i - \theta) - \rho(\hat{\theta}_i) \rho(\theta) \cos(\hat{\theta}_i - \theta) \right), \\
\frac{\partial M}{\partial \rho''(\hat{\theta}_i)} &= -\frac{1}{2\pi(D_\tau[\rho])^2} \frac{\partial \kappa_\rho(\hat{\theta}_i)}{\partial \rho''(\hat{\theta}_i)} \left(\rho^2(\theta) + \rho(\hat{\theta}_i) \rho'(\theta) \sin(\hat{\theta}_i - \theta) - \rho(\hat{\theta}_i) \rho(\theta) \cos(\hat{\theta}_i - \theta) \right)
\end{aligned}$$

where by (4.9)

$$\frac{\partial D_\tau[\rho]}{\partial \rho(\theta)} = \frac{\rho(\theta) - \rho(\hat{\theta}_i) \cos(\hat{\theta}_i - \theta)}{D_\tau[\rho]}, \quad \frac{\partial D_\tau[\rho]}{\partial \rho(\hat{\theta}_i)} = \frac{\rho(\hat{\theta}_i) - \rho(\theta) \cos(\hat{\theta}_i - \theta)}{D_\tau[\rho]},$$

and by (4.10)

$$\begin{aligned}
\frac{\partial \kappa_\rho}{\partial \rho} &= \frac{-\rho^3 - 4\rho(\rho')^2 + 2\rho^2\rho'' - \rho''(\rho')^2}{[\rho^2 + (\rho')^2]^{\frac{5}{2}}}, \\
\frac{\partial \kappa_\rho}{\partial \rho'} &= \frac{\rho'[\rho^2 - 2(\rho')^2 + 3\rho\rho'']}{[\rho^2 + (\rho')^2]^{\frac{5}{2}}}, \quad \text{and} \quad \frac{\partial \kappa_\rho}{\partial \rho''} = \frac{-\rho}{[\rho^2 + (\rho')^2]^{\frac{3}{2}}}.
\end{aligned}$$

Notice that

$$D_\tau[\rho] \geq \tau > 0,$$

the singular point $r = 0$ for $G_1(r)$, $G'_1(r)$, $Q(r)$, $Q'(r)$, $1/r^2$, and $1/r^3$ are not present in the above expression. Hence all the first-order derivatives of M are bounded. Similarly, we can take another derivative to prove that all the second-order derivatives are also bounded. On the other hand, $\nabla_{\mathcal{X}} \rho(\theta)$, $\nabla_{\mathcal{X}} \rho'(\theta)$, and $\nabla_{\mathcal{X}} \rho''(\theta)$ in (5.10) are computed by

$$\begin{aligned}
\nabla_{\mathcal{X}} \rho(\theta) &= \left(\cdots, \frac{\partial \rho(\theta)}{\partial a_i}, \cdots, \frac{\partial \rho(\theta)}{\partial b_i}, \cdots, \frac{\partial \rho(\theta)}{\partial c_i}, \cdots, \frac{\partial \rho(\theta)}{\partial d} \right), \\
\nabla_{\mathcal{X}} \rho'(\theta) &= \left(\cdots, \frac{\partial \rho'(\theta)}{\partial a_i}, \cdots, \frac{\partial \rho'(\theta)}{\partial b_i}, \cdots, \frac{\partial \rho'(\theta)}{\partial c_i}, \cdots, \frac{\partial \rho'(\theta)}{\partial d} \right),
\end{aligned}$$

$$\nabla_{\mathcal{X}} \rho''(\theta) = \left(\cdots, \frac{\partial \rho''(\theta)}{\partial a_i}, \cdots, \frac{\partial \rho''(\theta)}{\partial b_i}, \cdots, \frac{\partial \rho''(\theta)}{\partial c_i}, \cdots, \frac{\partial \rho''(\theta)}{\partial d} \right).$$

From (5.6), (5.7), as well as (5.8), we deduce

$$\begin{aligned} \frac{\partial \rho(\theta)}{\partial a_i} &= \Psi(b_i \theta + c_i), & \frac{\partial \rho(\theta)}{\partial b_i} &= a_i \theta \Psi'(b_i \theta + c_i), \\ \frac{\partial \rho(\theta)}{\partial c_i} &= a_i \Psi'(b_i \theta + c_i), & \frac{\partial \rho(\theta)}{\partial d} &= 1; \\ \frac{\partial \rho'(\theta)}{\partial a_i} &= b_i \Psi'(b_i \theta + c_i), & \frac{\partial \rho'(\theta)}{\partial b_i} &= a_i \Psi'(b_i \theta + c_i) + a_i b_i \theta \Psi''(b_i \theta + c_i), \\ \frac{\partial \rho'(\theta)}{\partial c_i} &= a_i b_i \Psi''(b_i \theta + c_i), & \frac{\partial \rho'(\theta)}{\partial d} &= 0; \\ \frac{\partial \rho''(\theta)}{\partial a_i} &= b_i^2 \Psi''(b_i \theta + c_i), & \frac{\partial \rho''(\theta)}{\partial b_i} &= 2a_i b_i \Psi''(b_i \theta + c_i) + a_i b_i^2 \theta \Psi'''(b_i \theta + c_i), \\ \frac{\partial \rho''(\theta)}{\partial c_i} &= a_i b_i^2 \Psi'''(b_i \theta + c_i), & \frac{\partial \rho''(\theta)}{\partial d} &= 0. \end{aligned}$$

Similar calculations also work for $\nabla_{\mathcal{X}} \rho(\hat{\theta}_i)$, $\nabla_{\mathcal{X}} \rho'(\hat{\theta}_i)$, and $\nabla_{\mathcal{X}} \rho''(\hat{\theta}_i)$. Since the activation function $\Psi \in C^4$ in our assumptions, $\nabla_{\mathcal{X}} \rho$, $\nabla_{\mathcal{X}} \rho'$, and $\nabla_{\mathcal{X}} \rho''$ are all bounded. In the same manner, we can calculate second derivative of ρ , ρ' , and ρ'' , namely, the Hessian functions $\nabla_{\mathcal{X}}^2 \rho, \nabla_{\mathcal{X}}^2 \rho', \nabla_{\mathcal{X}}^2 \rho'' : \mathbb{R}^d \rightarrow \mathbb{R}^{d \times d}$. We shall find that $\nabla_{\mathcal{X}}^2 \rho, \nabla_{\mathcal{X}}^2 \rho', \nabla_{\mathcal{X}}^2 \rho''$ contain at most fourth-order derivative of Ψ , hence they are all bounded as $\Psi \in C^4$.

Combining the above analysis, we find that $\nabla_{\mathcal{X}} F(\mathcal{X}, \hat{\theta})$ is bounded. To further claim that it is Lipschitz continuous, we take another derivative with respect to \mathcal{X} to derive

$$\begin{aligned} \nabla_{\mathcal{X}}^2 F(\mathcal{X}, \hat{\theta}) &= \frac{2}{m} \sum_{i=1}^m \left[(\nabla_{\mathcal{X}} \mathcal{L}_{\tau}[\rho](\hat{\theta}_i))^T \nabla_{\mathcal{X}} \mathcal{L}_{\tau}[\rho](\hat{\theta}_i) + (\mathcal{L}_{\tau}[\rho](\hat{\theta}_i)) \nabla_{\mathcal{X}}^2 \mathcal{L}_{\tau}[\rho](\hat{\theta}_i) \right] \\ &\quad + 2 \sum_{\alpha=0}^2 \left(\nabla_{\mathcal{X}} (D^{\alpha}(\rho(0; \mathcal{X}) - \rho(2\pi; \mathcal{X}))) \right)^T \left(\nabla_{\mathcal{X}} (D^{\alpha}(\rho(0; \mathcal{X}) - \rho(2\pi; \mathcal{X}))) \right) \\ &\quad + 2 \sum_{\alpha=0}^2 \left(D^{\alpha}(\rho(0; \mathcal{X}) - \rho(2\pi; \mathcal{X})) \right) \left(\nabla_{\mathcal{X}}^2 (D^{\alpha}(\rho(0; \mathcal{X}) - \rho(2\pi; \mathcal{X}))) \right), \end{aligned}$$

where by (5.9) and (5.10),

$$\begin{aligned} \nabla_{\mathcal{X}}^2 \mathcal{L}_{\tau}[\rho](\hat{\theta}_i) &= \int_0^{2\pi} \nabla_{\mathcal{X}}^2 M(\theta, \hat{\theta}_i) d\theta, \\ \nabla_{\mathcal{X}}^2 M &= \frac{\partial^2 M}{\partial \rho(\theta)^2} (\nabla_{\mathcal{X}} \rho(\theta))^T \nabla_{\mathcal{X}} \rho(\theta) + \frac{\partial M}{\partial \rho(\theta)} \nabla_{\mathcal{X}}^2 \rho(\theta) + 2 \frac{\partial^2 M}{\partial \rho(\theta) \partial \rho(\hat{\theta}_i)} (\nabla_{\mathcal{X}} \rho(\theta))^T \nabla_{\mathcal{X}} \rho(\hat{\theta}_i) + \cdots. \end{aligned}$$

According to the above analysis, each term in the above formula for $\nabla_{\mathcal{X}}^2 F(\mathcal{X}, \hat{\theta})$ is bounded, hence $\nabla_{\mathcal{X}} F(\mathcal{X}, \hat{\theta})$ is Lipschitz continuous in \mathcal{X} . Using (5.4), we conclude that the objective gradient function $\nabla_{\mathcal{X}} J(\mathcal{X})$ is also Lipschitz continuous.

5.2. First and second moment limits. Next, we shall prove the first and second moment limits condition in [45]. The proof can be justified in three parts:

(a) According to our assumptions in Theorem 5.1, $\{\mathcal{X}_k\}$ is contained in an open set which is bounded. From 4.1, $J(\mathcal{X})$ is continuously differentiable, hence $J(\mathcal{X}_k)$ is clearly bounded.

(b) Since $G(\mathcal{X}_k, \hat{\theta}_k) = \nabla_{\mathcal{X}} F(\mathcal{X}_k, \hat{\theta}_k)$, we have

$$\mathbb{E}_{\hat{\theta}_k}[G(\mathcal{X}_k, \hat{\theta}_k)] = \mathbb{E}_{\hat{\theta}_k}[\nabla_{\mathcal{X}} F(\mathcal{X}_k, \hat{\theta}_k)] = \nabla_{\mathcal{X}} \left(\mathbb{E}_{\hat{\theta}_k}[F(\mathcal{X}_k, \hat{\theta}_k)] \right) = \nabla_{\mathcal{X}} J(\mathcal{X}_k).$$

Therefore,

$$\nabla_{\mathcal{X}} J(\mathcal{X}_k)^T \mathbb{E}_{\hat{\theta}_k}[G(\mathcal{X}_k, \hat{\theta}_k)] = \nabla_{\mathcal{X}} J(\mathcal{X}_k)^T \cdot \nabla_{\mathcal{X}} J(\mathcal{X}_k) = \|\nabla_{\mathcal{X}} J(\mathcal{X}_k)\|_2^2.$$

It then directly follows that

$$\nabla_{\mathcal{X}} J(\mathcal{X}_k)^T \mathbb{E}_{\hat{\theta}_k}[G(\mathcal{X}_k, \hat{\theta}_k)] \geq u \|\nabla_{\mathcal{X}} J(\mathcal{X}_k)\|_2^2,$$

and $\|\mathbb{E}_{\hat{\theta}_k}[G(\mathcal{X}_k, \hat{\theta}_k)]\|_2 = \|\nabla_{\mathcal{X}} J(\mathcal{X}_k)\|_2 \leq u_G \|\nabla_{\mathcal{X}} J(\mathcal{X}_k)\|_2$
hold true for some $0 < u \leq 1$ and $u_G \geq 1$.

(c) Based on the analysis in 4.1, we know that $G(\mathcal{X}_k, \hat{\theta}_k) = \nabla_{\mathcal{X}} F(\mathcal{X}_k, \hat{\theta}_k)$ is bounded for each k , hence $\mathbb{E}_{\hat{\theta}_k}[\|G(\mathcal{X}_k, \hat{\theta}_k)\|_2^2]$ is also bounded. Since

$$\mathbb{V}_{\hat{\theta}_k}[G(\mathcal{X}_k, \hat{\theta}_k)] = \mathbb{E}_{\hat{\theta}_k}[\|G(\mathcal{X}_k, \hat{\theta}_k)\|_2^2] - \|\mathbb{E}_{\hat{\theta}_k}[G(\mathcal{X}_k, \hat{\theta}_k)]\|_2^2 \leq \mathbb{E}_{\hat{\theta}_k}[\|G(\mathcal{X}_k, \hat{\theta}_k)\|_2^2],$$

it indicates that $\mathbb{V}_{\hat{\theta}_k}[G(\mathcal{X}_k, \hat{\theta}_k)]$ is bounded.

We have verified the two sufficient assumptions in [45]. Using the Theorem 4.10 in [45], with the diminishing step-size, i.e.,

$$\sum_{k=1}^{\infty} \alpha_k = \infty \quad \text{and} \quad \sum_{k=1}^{\infty} \alpha_k^2 < \infty,$$

we get the convergence result,

$$\mathbb{E}\left[\frac{1}{A_k} \sum_{k=1}^K \alpha_k \|\nabla F(\mathcal{X})\|_2^2\right] \rightarrow 0 \quad \text{as } K \rightarrow \infty. \quad \square$$

The stochastic gradient decent method generates critical points. We are only interested in those critical points whose loss function is close to zero, hence generating an approximate solution to our free boundary problem – this is achieved in our numerical examples.

6. NUMERICAL RESULTS

6.1. Verification of the neural network discretization near bifurcation points. Near the bifurcation points $\mu = \mu_n(R_s)$, the shape of the symmetry-breaking free boundary is fully characterized by Theorem 2.1 (see also Remark 2.1). In this section we show that all these free boundary solutions can be fully recovered by the neural network discretization. In particular, we compute the numerical solution with Algorithm 1 near the bifurcation points μ_n by (2.16) with $R_S = 1$, namely,

$$\mu_2 \approx 14.7496, \quad \mu_3 \approx 28.7234, \quad \mu_4 \approx 47.1794, \quad \mu_5 \approx 70.1169.$$

We choose μ in a small neighborhood of μ_n , i.e., $|\mu - \mu_n|$ is small; correspondingly, $\beta = (\mu + 1) \frac{I_1(1)}{I_0(1)}$ is uniquely determined by (2.6). For the neural network discretization, we set the number of neurons $N = 20$, the number of Monte Carlo integration points $m = 4000$, $\tau = 10^{-3}$, the maximum number of iterations as 50, learning rate $= 10^{-4}$, and the activation function $\Psi(\theta) = \cos(\theta)$. The initial parameters are set to be: a_i is randomly chosen by $N(0, 1)$, $b_i = n$ (which corresponds to the n -mode bifurcation), $c_i = 0$, and $d = 1$; in this way, the Neural network representation $\rho(\theta, \mathcal{X}) = \sum_{i=1}^N a_i \Psi(b_i \theta + c_i) + d$ is close to the form of free boundary for the symmetry-breaking solution (2.18). Moreover, $\hat{\theta}_i$ are uniformly sampled from $[0, 2\pi]$, and are divided into 20 mini-batches, with each mini-batch containing 200 points. Therefore, all the parameters are updated 20 times in one epoch. The loss is shown in Figure 1 while the shapes of symmetry-breaking solutions on different bifurcation branches are shown in Figure 2 which is consistent with the theoretical results in Theorem 2.1 and Remark 2.1.

6.2. New non-radially symmetric solutions. In this section we generate some non-radially symmetric solutions that are not characterized by any theorems. Inspired by [46], we try to find some fingering patterns, hence we choose the activation function $\Psi(\theta) = 0.3/[(\cos(\theta))^2 + (0.3 \sin(\theta))^2]$, which generates fingering-like patterns. In particular, we take $\mu = 20$, $\beta = (\mu + 1) \frac{I_1(1)}{I_0(1)}$, $N = 20$, $m = 10000$, $\tau = 10^{-3}$ and maximum number of iterations $= 200$. We divide 10000 random points $\hat{\theta}_i$ into 100 mini-batches, hence all the parameters are updated 100 times in one iteration.

In Figure 3, we initially choose $b_i = 1$ and randomly choose other parameters. The learning rate is 10^{-3} at first and is decreased gradually to 10^{-6} . In Figure 4, we take $b_i = 2$, $c_i = 0$, random a_i , a random d , and a 10^{-5} learning rate. Compared with Figure 1, the loss in Figures 3 and 4 are larger. It is due to the numerical error introduced by calculating the curvature at the tip of each finger and the connecting points between two adjacent fingers.

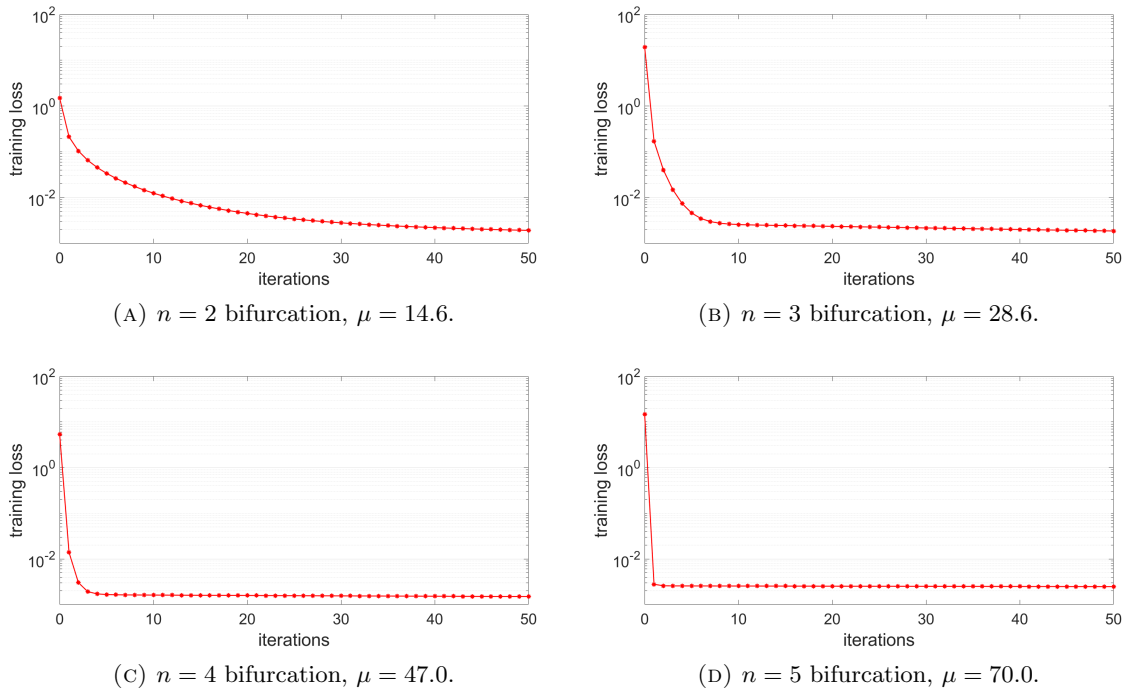


FIGURE 1. Training loss.

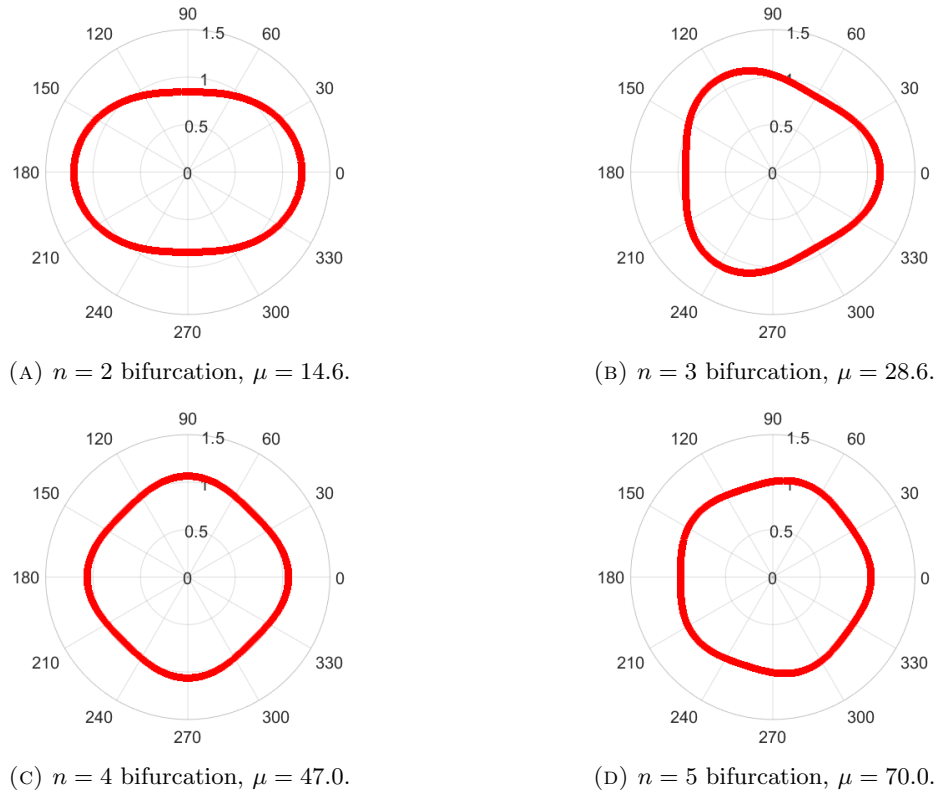


FIGURE 2. Contour plot of non-radially symmetric solutions in different bifurcation branches.

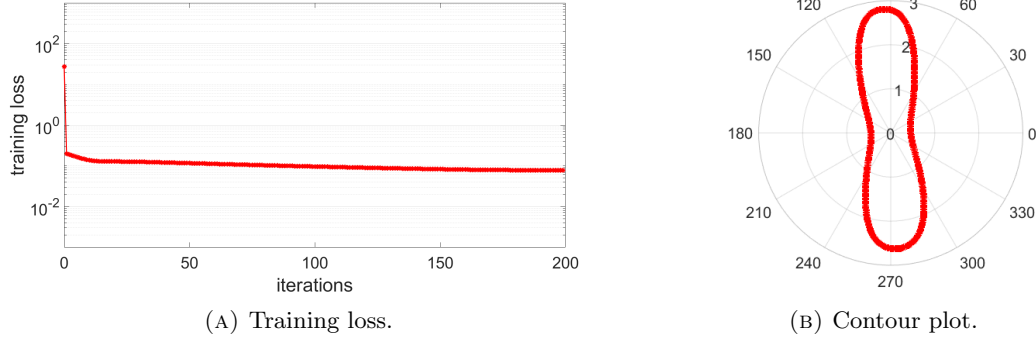


FIGURE 3. Non-radially symmetric solution with 2 fingers.

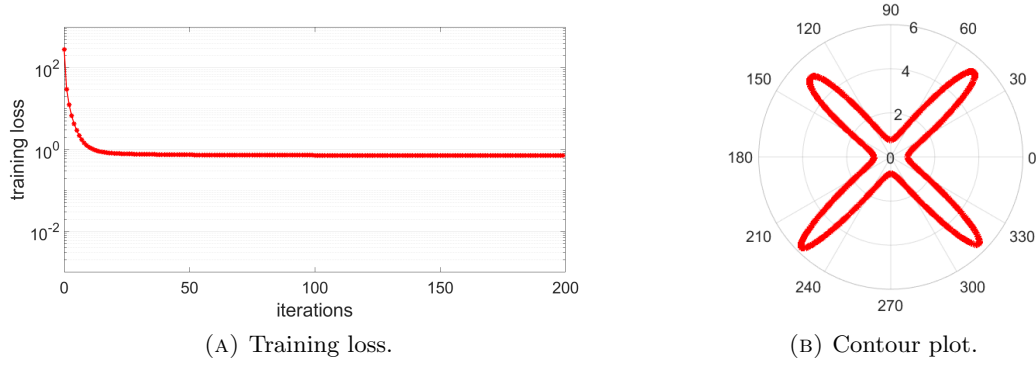


FIGURE 4. Non-radially symmetric solution with 4 fingers.

7. CONCLUSION

We have developed a novel numerical method based on the neural network discretization for solving a modified Hele-Shaw model of PDE free boundary problem. We established theoretically the existence of the numerical solution with this new discretization. Our simulations verify this new approach on radially symmetric and known non-radially symmetric solutions. Moreover, using this new method, we also found some new non-radially symmetric solutions that were unknown based on the existing theories. In the future, we will apply this new numerical method to solve the more sophisticated free boundary problems such as tumor growth models or the atherosclerotic plaque formation models.

8. APPENDIX

Theorem 8.1. (Crandall-Rabinowitz theorem, [47]) *Let X, Y be real Banach spaces and $F(\cdot, \cdot)$ a C^p map, $p \geq 3$, of a neighborhood $(0, \mu_0)$ in $X \times \mathbb{R}$ into Y . Suppose*

- (1) $F(0, \mu) = 0$ for all μ in a neighborhood of μ_0 ,
- (2) $\text{Ker } F_x(0, \mu_0)$ is one dimensional space, spanned by x_0 ,
- (3) $\text{Im } F_x(0, \mu_0) = Y_1$ has codimension 1,
- (4) $F_{\mu x}(0, \mu_0)x_0 \notin Y_1$.

Then $(0, \mu_0)$ is a bifurcation point of the equation $F(x, \mu) = 0$ in the following sense: In a neighborhood of $(0, \mu_0)$ the set of solutions $F(x, \mu) = 0$ consists of two C^{p-2} smooth curves Γ_1 and Γ_2 which intersect only at the point $(0, \mu_0)$; Γ_1 is the curve $(0, \mu)$ and Γ_2 can be parameterized as follows:

$$\Gamma_2 : (x(\varepsilon), \mu(\varepsilon)), |\varepsilon| \text{ small}, (x(0), \mu(0)) = (0, \mu_0), x'(0) = x_0.$$

REFERENCES

- [1] A. Friedman. Free boundary problems in biology. *Phil. Trans. R. Soc. A*, 373(2050):20140368, 2015.
- [2] A. Friedman and W. Hao. A mathematical model of atherosclerosis with reverse cholesterol transport and associated risk factors. *Bulletin of mathematical biology*, 77(5):758–781, 2015.
- [3] W. Hao, E. Crouser, and A. Friedman. Mathematical model of sarcoidosis. *Proceedings of the National Academy of Sciences*, 111(45):16065–16070, 2014.
- [4] W. Hao and A. Friedman. The ldl-hdl profile determines the risk of atherosclerosis: a mathematical model. *PloS one*, 9(3):e90497, 2014.
- [5] W. Hao, J. Hauenstein, B. Hu, and A. Sommesse. A three-dimensional steady-state tumor system. *Applied Mathematics and Computation*, 218(6):2661–2669, 2011.
- [6] A. Friedman and J. Spruck. *Variational and free boundary problems*, volume 53. Springer Science & Business Media, 2012.
- [7] P. Saffman and G. Taylor. The penetration of a fluid into a porous medium or hele-shaw cell containing a more viscous liquid. *Proceedings of the Royal Society of London. Series A. Mathematical and Physical Sciences*, 245(1242):312–329, 1958.
- [8] H. Hele-Shaw. Flow of water. *Nature*, 58:520, 1898.
- [9] X. Chen and A. Friedman. A free boundary problem for an elliptic-hyperbolic system: an application to tumor growth. *SIAM Journal on Mathematical Analysis*, 35(4):974–986, 2003.
- [10] E. DiBenedetto and A. Friedman. The ill-posed hele-shaw model and the stefan problem for supercooled water. *Transactions of the American Mathematical Society*, 282(1):183–204, 1984.
- [11] P. Constantin and M. Pugh. Global solutions for small data to the hele-shaw problem. *Nonlinearity*, 6(3):393, 1993.
- [12] W. Hao, J. Hauenstein, B. Hu, T. McCoy, and A. Sommesse. Computing steady-state solutions for a free boundary problem modeling tumor growth by stokes equation. *Journal of Computational and Applied Mathematics*, 237(1):326–334, 2013.
- [13] Y. Wang, W. Hao, and G. Lin. Two-level spectral methods for nonlinear elliptic equations with multiple solutions. *SIAM Journal on Scientific Computing*, 40(4):B1180–B1205, 2018.
- [14] W. Hao, J. Hauenstein, B. Hu, Y. Liu, A. Sommesse, and Y.-T. Zhang. Bifurcation for a free boundary problem modeling the growth of a tumor with a necrotic core. *Nonlinear Analysis: Real World Applications*, 13(2):694–709, 2012.
- [15] W. Hao, B. Hu, and A. Sommesse. Numerical algebraic geometry and differential equations. In *Future Vision and Trends on Shapes, Geometry and Algebra*, pages 39–53. Springer, 2014.
- [16] W. Hao, J. Hesthaven, G. Lin, and B. Zheng. A homotopy method with adaptive basis selection for computing multiple solutions of differential equations. *Journal of Scientific Computing*, 82(1):19, 2020.
- [17] W. Hao and S. Zhu. Parallel iterative methods for parabolic equations. *International Journal of Computer Mathematics*, 86(3):431–440, 2009.
- [18] W. Hao, B. Hu, S. Li, and L. Song. Convergence of boundary integral method for a free boundary system. *Journal of Computational and Applied Mathematics*, page submitted, 2015.
- [19] N. Sebe, I. Cohen, A. Garg, and T. Huang. *Machine learning in computer vision*, volume 29. Springer Science & Business Media, 2005.
- [20] F. Camastra and A. Vinciarelli. *Machine learning for audio, image and video analysis: theory and applications*. Springer, 2015.
- [21] N. Indurkha and F. Damerau. *Handbook of natural language processing*. Chapman and Hall/CRC, 2010.
- [22] D. Amodei, S. Ananthanarayanan, and R. Anubhai. Deep speech 2: End-to-end speech recognition in english and mandarin. In *International conference on machine learning*, pages 173–182, 2016.
- [23] I. Bright, G. Lin, and J. N. Kutz. Compressive sensing based machine learning strategy for characterizing the flow around a cylinder with limited pressure measurements. *Physics of Fluids*, 25(12):127102, 2013.
- [24] M. Raissi, P. Perdikaris, and G. Karniadakis. Machine learning of linear differential equations using gaussian processes. *Journal of Computational Physics*, 348:683–693, 2017.
- [25] P. Dillenbourg. *Collaborative learning: Cognitive and computational approaches. advances in learning and instruction series*. ERIC, 1999.
- [26] S. Durrleman, M. Prastawa, N. Charon, J. Korenberg, S. Joshi, G. Gerig, and A. Trouvé. Morphometry of anatomical shape complexes with dense deformations and sparse parameters. *NeuroImage*, 101:35–49, 2014.
- [27] H. Yang. *Oscillatory data analysis and fast algorithms for integral operators*. PhD thesis, Stanford University, 2015.
- [28] S. Marsland. *Machine learning: an algorithmic perspective*. CRC press, 2015.
- [29] Yaodan Huang, Zhengce Zhang, and Bei Hu. Bifurcation for a free-boundary tumor model with angiogenesis. *Nonlinear Analysis: Real World Applications*, 35:483–502, 2017.
- [30] F. Li and B. Liu. Bifurcation for a free boundary problem modeling the growth of tumors with a drug induced nonlinear proliferation rate. *Journal of Differential Equations*, 263:7627–7646, 2017.
- [31] Avner Friedman and Bei Hu. Bifurcation from stability to instability for a free boundary problem arising in a tumor model. *Archive for rational mechanics and analysis*, 180(2):293–330, 2006.
- [32] H. Pan and R. Xing. Bifurcation for a free boundary problem modeling tumor growth with ECM and MDE interactions. *Nonlinear Analysis: Real World Applications*, 43:362–377, 2018.
- [33] Z. Wang. Bifurcation for a free boundary problem modeling tumor growth with inhibitors. *Nonlinear Analysis: Real World Applications*, 19:45–53, 2014.

- [34] Xinyue Evelyn Zhao and Bei Hu. Symmetry-breaking bifurcation for a free-boundary tumor model with time delay. *Journal of Differential Equations*, 269:1829–1862, 2020.
- [35] Andrei Borisovich and Avner Friedman. Symmetry-breaking bifurcations for free boundary problems. *Indiana University mathematics journal*, pages 927–947, 2005.
- [36] Prasanta Kumar Banerjee and Roy Butterfield. *Boundary element methods in engineering science*, volume 17. McGraw-Hill London, 1981.
- [37] Henry Power and Luiz C Wrobel. *Boundary integral methods in fluid mechanics*. Computational mechanics, 1995.
- [38] Kara Pham, Emma Turian, Kai Liu, Shuwang Li, and John Lowengrub. Nonlinear studies of tumor morphological stability using a two-fluid flow model. *Journal of mathematical biology*, 77(3):671–709, 2018.
- [39] Vittorio Cristini, John Lowengrub, and Qing Nie. Nonlinear simulation of tumor growth. *Journal of mathematical biology*, 46(3):191–224, 2003.
- [40] Avner Friedman. *Generalized functions and partial differential equations*. Courier Corporation, 2005.
- [41] Rainer Kress, V Maz'ya, and V Kozlov. *Linear integral equations*, volume 82. Springer, 1989.
- [42] Wenrui Hao, Bei Hu, Shuwang Li, and Lingyu Song. Convergence of boundary integral method for a free boundary system. *Journal of Computational and Applied Mathematics*, 334:128–157, 2018.
- [43] Kurt Hornik. Approximation capabilities of multilayer feedforward networks. *Neural networks*, 4(2):251–257, 1991.
- [44] Milton Abramowitz and Irene A Stegun. *Handbook of mathematical functions with formulas, graphs, and mathematical tables*, volume 55. US Government printing office, 1948.
- [45] Léon Bottou, Frank E Curtis, and Jorge Nocedal. Optimization methods for large-scale machine learning. *Siam Review*, 60(2):223–311, 2018.
- [46] José A Miranda and Enrique Alvarez-Lacalle. Viscosity contrast effects on fingering formation in rotating hele-shaw flows. *Physical Review E*, 72(2):026306, 2005.
- [47] M.G. Grandall and P.H. Rabinowitz. Bifurcation from simple eigenvalues. *Journal of Functional Analysis*, 8:321–340, 1971.

DEPARTMENT OF APPLIED AND COMPUTATIONAL MATHEMATICS AND STATISTICS,, UNIVERSITY OF NOTRE DAME, NOTRE DAME, IN 46556, USA, xzhao6@ND.EDU

DEPARTMENT OF MATHEMATICS,, THE PENNSYLVANIA STATE UNIVERSITY, UNIVERSITY PARK, PA 16802, USA, wxh64@PSU.EDU

DEPARTMENT OF APPLIED AND COMPUTATIONAL MATHEMATICS AND STATISTICS,, UNIVERSITY OF NOTRE DAME, NOTRE DAME, IN 46556, USA, b1hu@ND.EDU